Quantum Mechanical Investigation of Carbazole-Coumarine Hybrid Interactions with TiO_2 in organic Dye-Sensitized Solar Cell

BY

HIZB ULLAH KHAN

Reg. # 00000203340

2017-NUST-MS-CS&E-10

A treatise Submitted in the partial fulfillment of the Requirement for the Degree of Master of Science (MS)

IN

Computational Science and Engineering

Supervisor

Dr. Fouzia Malik

Research Centre for Modelling and Simulation (RCMS) National University of Sciences and Technology (NUST)

Islamabad, Pakistan (2021)

Dedicated

To

My Family

Statement of Originality

I hereby proclaim that my thesis work titles "Quantum Mechanical Investigation of Carbazole-Coumarine Hybrid Interactions with Iodide in organic Dye-Sensitized Solar Cell" is carried out by me under the supervision of Dr. Fouzia Malik at the Research Center for Modeling and Simulation (RCMS) at the National University of Sciences and Technology (NUST). I solemnly affirm that to the best of my knowledge, this is my original work and it contains no material which has been accepted for the award of other degrees in my name, in any other university. Also, no material previously published or written by any other person has been included in this thesis except where due reference has been made to the previously published work.

Hizb Ullah Khan

MS Computational Science & Engineering

Acknowledgments

All praise and glory to **ALLAH SUBHANA'O TAALA** the only creator who helped and guided me in all fields of life. All the respect for **HOLY PROPHET HAZRAT MUHAMMAD (P.B.U.H**) whose life is an ideal pattern of success for us.

I feel great inclination and prerogative to express my intense sense of gratitude and earnest obligations to my worthy supervisor Dr. Fouzia Malik Associate Professor, Research Center for Modeling and Simulation (RCMS), National University of Sciences and Technology (NUST) for her continuous support, supervision throughout my course work and research work. She gave me the autonomy to define my research and my thoughts. Whenever I was deprived of ideas, my communication with her always helped me get back on the right pathway. She has always fortified me to pursue more, to full fill dreams, and also helped me to explore wonderful moments during research.

I am thankful to GEC members – Dr. Rehan Zafar Paracha, RCMS, NUST, Dr. Tayyaba Noor, SCME, NUST, Dr. Zamir Hussain, RCMS, NUST. I am also very grateful to Dr. Humaira Rafique UOG, Gujrat for giving me valuable suggestions, collaboration, and support during my research. It would be negligent not to mention the names of Engr. Muhammad Usman and Engr. Muhammad Hassan for their assistance at Super-Computing Lab RCMS, NUST. I would like to give special thanks to Dr. Muizuddin Shami (Principle RCMS), Dr. Ishrat Jabeen (H.O.D RCMS), and all my teachers at RCMS, Lab fellows especially Haris Bin Tanveer, Farhan Ullah, Zeeshan Khan M. Younas Khan for their support during all my stay at RCMS.

On a personal note, I know that this work could not have been completed without the tremendous support of my friends and family. Finally, my gratitude to my parents is beyond measure, they always sacrificed themselves to ensure that I had the best opportunities possible and they have constantly believed in me and encouraged me to break boundaries and pursue my dreams. Their support has meant to me over the years and I dedicate this thesis to them.

Hizb Ullah Khan

List of Contents

List of Abbreviations

ADF	Amsterdam Density Functional
CB	Conduction Band
DFT	Density Functional Theory
DOS	Density of states
DSSC	Dye-Sensitized Solar Cell
GGA	Gradient generalized approximation
HOMO	Highest Occupied Molecular Orbital
LDA	Local density approximation
LUMO	Lowest Unoccupied Molecular Orbital
NIR	Nuclear Infra-red
PCE	Photo-electric Conversion
PES	Potential Energy Surfaces
PV	Photovoltaic
UV	Ultra Violet
Vis	Visible

List of Tables

List of Figures

ABSTRACT

Due to the flexibility, limpidity, and high proficiency compared to conventional inorganic solar cells, dye-sensitized solar cells (DSSCs) have received much attention in past years. DSSCs are serene of mostly non-toxic constituents and might be made up without exclusive and energy-intensive high temperature and high vacuum procedures. In this thesis, we have investigated the heterogeneous adsorption mechanism of five novel dyes of coumarins namely 6, 8-Dimethoxy-7-methyl-3-phenylisocoumarin, 6, 8-Dimethoxy-7-methyl-3-(p-tolyl) isocoumarin, 6, 8-Dimethoxy-7-methyl-3-(4'-methoxyphenyl) isocoumarin, 6, 8-Dimethoxy-7-methyl-3-(4'-chlorophenyl) isocoumarin, 6, 8-Dimethoxy-7-methyl-3-(4'-nitrophenyl) isocoumarin, and a single carbazole namely, 3,5-dinitro-N-octylcarbazole with titanium dioxide (TiO_2) to determine the adsorption prosperity based on computational studies. Based on quantum chemical findings calculated adsorption energy was found more favorable for 6, 8-Dimethoxy-7-methyl-3-(4'-chlorophenyl) isocoumarin as compared to the other four isocoumarin dyes due to the presence of the Cl group possessing electron-donating capability and having a more negative value of adsorption energy i.e., -7.128×10^3eV. On the other hand, a heterogeneous adsorption mechanism was also considered for five hybrids of isocoumarin and a carbazole dye (HK-1), (HK-2), (HK-3), (HK-4), (HK-5), to determine the electron transfer and injection phenomenon based on computational studies. Among all five hybrid dyes (HK-3) showed the greatest efficiency of electron injection from E_{LUMO} of the hybrid into the conduction band of nanocrystalline TiO_2 in DSSC. The results revealed that hybrids show high efficiency to inject the electron into the conduction band of TiO_2 leading to oxidation of dye-hybrids and transfer and diffusion of the electron to counter electrode. Results demonstrated that electron injection efficiency increased in the presence of dye-hybrids as a photosensitizer.

Chapter 1

INTRODUCTION

Introduction

1.1 Background

Energy has been one of the fundamental needs of living in the new era of technological advances. If the global population rises, the energy demand also increases. In the next three decades, worldwide electricity demand needs to double; this is impossible to occur with insufficient reserves of fossil fuels. Nuclear technology is proved guilty of protection and waste disposal problems as it can provide large-scale power. Up till now, fossil fuels have been the primary source of most global energy supply, and in addition to being non-renewable, emit vast amounts of carbon dioxide, the greenhouse gas that is a major hazard to the world's biodiversity.

It is expected that global energy demand will rise by almost 70% between 2000 and 2030. Fossil fuels, which produce 80 % of the energy utilized globally, are rapidly depleting in terms of resources. In 2002, the world's fossil fuel reserves were predicted to last 40 years for oil, 60 years for natural gas, and 200 years for coal. Because of rising energy consumption, depletion of fossil resources, global warming, and the attendant climate change, there is an urgent need for environmentally sustainable energy technology [1]–[4]

Pakistan’s energy sector remains one of the main objects to economic growth. Though Pakistan has succeeded to increase electricity generation since 2013 and mitigate the country's electricity blackouts in the past decade, expensive fuels, reliance on imported energy products, chronic gas shortages and electricity, heavy energy debt, aging, and inadequate transmission and distribution systems have prevented the industry from growing. Pakistan's overall installed power generation capacity is 39,000 megawatts, of which 66% comes from thermal (fossil) sources, 24% from hydro and 6% from renewable energy (wind, solar and nuclear), and 4% from nuclear energy, according to the 2019 Annual National Electric Regulatory Authority (NEPRA). Renewable energy (RE) resources may play a significant role in closing the gap in the current scenario [5]–[9].

Alternative energy tools including photovoltaic solar energies, solar temperature energies, biofuels, and renewable coal production could be utilized to satisfy the present and future

demand to generate clean electricity. Solar energy tends to be an enticing clean alternative source of energy among renewable resources that can help us boost our energy independence and reduce the impact of global warming. The use of the available solar energy is one of the easiest ways to minimize the use of fossil fuels and thereby reduce carbon emissions. While the potential of solar energy for mitigating carbon and for providing deemed electricity to customers is high, solar energy has accounted for a relatively small percentage of the overall energy generated and renewable energy sources due to the high cost of capital [10]–[13].

1.2 Solar Cell Technology

A solar cell or photovoltaic (PV) cell is an electrical device that transforms light power, which is a physical and chemical phenomenon, directly into electricity through a photovoltaic effect. The photovoltaic effect was observed by Becquerel in 1839, which is a theoretical objective of solar energy use. Every single hour the energy absorption from the sun by the Earth's atmosphere is more than adequate for the whole year to fulfill global energy needs. For this cause, technology has erupted in recent decades to find the most powerful and cost-effective solar cells to keep the planet from becoming dependent on fossil fuels. Solar energy is a natural fuel available worldwide. Solar PV technology, as opposed to many other electric generation systems, is very related and can be used almost anywhere. In comparison to traditional coal, nuclear, petrol, and gas power stations, solar PV is free of fuel and comparatively low cost of operations and maintenance (O&M) [14]–[17].

1.2.1 Physics of Solar Cell

Photovoltaic instruments operate on the phenomena of charge separation arising at the interface of two separate materials. These materials have different mechanisms of conduction. The direct transformation of solar radiation into electrical power can be represented by solar Photovoltaic. The photoelectric materials absorb energy in the form of photons of light and emit free electrons. The isolation or flow of these free electrons contributes to the production of electric current.

The working of a solar cell can be divided into three simple steps:

- Adsorption of light
- Charge separation
- Charge collection

Due to these basic steps, the chemical and physical processes in various cell types vary and depend on the materials used. The efficiency of each step determines solar cell efficiency. The selection of suitable cell design materials will optimize performance. Semiconductor wafer typically produces an electric field if approached to form a positive and a negative side (p and n junctions). Electrons are knocked out from semiconductor atoms as the solar cells are irradiated to light. The electric current is generated if the circuit is completed by touching electrical conductors connected to the two sides (positive and negative).

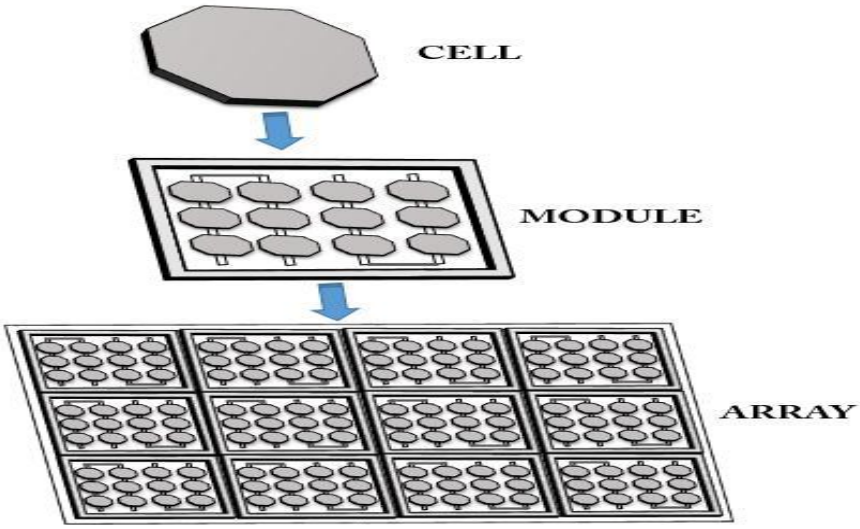

Fig. 1.1 Diagram showing a cell, module, and an array.

Many solar cells form the solar panel when they are placed on a frame or support and electrically attached. The current created by the module depends on the level of light that the module strikes and the module/array field. The modules are designed to supply a certain voltage of electricity. When connected, several modules form an array to generate electrical current. The created current is direct current [18]–[23].

1.2.2 Photovoltaics Performance

The electricity generation by a solar cell or panel is defined by current curves of density-voltage (JV) or current-tension (IV). Short circuit current (Jsc) is the maximum current generated when the cell is short-circuited and open-circuit voltage (Voc) is the maximum voltage when the cell is under an open circuit state. The electricity generated by a cell or panel is the function of the current density and voltage. The maximum output point of the IV (Pmax) curve is the point where the maximum output of the voltage and density of the current is the maximum in watts provided by the cell.

$$P_{max} = J_{mpp} \times V_{mpp}. \qquad (1)$$

Fill Factor is the ratio of maximum obtainable power to the product of Voc and Jsc.

$$FF = \frac{J_{mpp} \times V_{mpp}}{J_{sc} \times V_{oc}}. \qquad (2)$$

From the above equation (2) Pmax cab be written as:

$$P_{max} = J_{sc} \times V_{oc} \times FF. \qquad (3)$$

Although the various types of solar cells have different components and operating concepts, these characteristics are essential to assess their effectiveness in all types of solar cells [24].

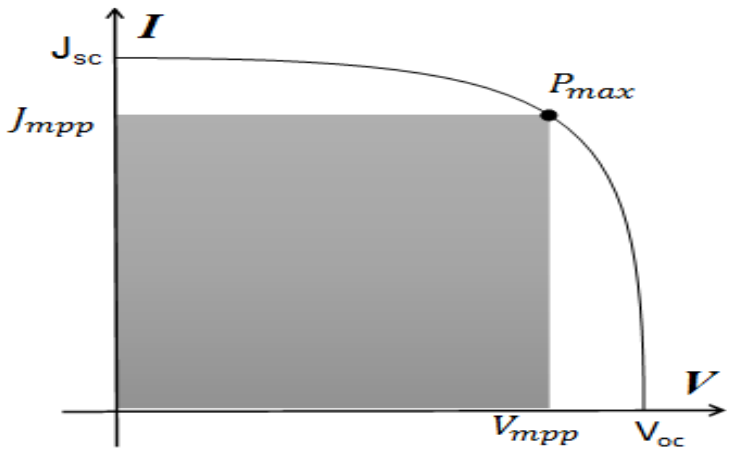

Fig 1.2: IV characteristics curve for solar cells.

The maximum cell power produced by incident light divided (W / m2) specifies the efficiency of the solar cell's energy conversion.

$$\eta = \frac{P_{max}}{P_{light}},$$

where η is the efficiency, P_{max} is the maximum power point and, P_{light} is the power of light.

The efficiency of solar cell's performance will be measured under normal tests, i.e., 1000W / m^2 irradiance, air mass 1.5 spectrum, and temperature 25 °C.

A general comparison between DSSCs and conventional solar cells is in **Table 1.1**:

1.1 Comparison table of conventional solar cells and dye-sensitized solar cells

Properties	Conventional solar cells	Dye-Sensitized Solar Cells
Power generation cost	High	Low
Power generation efficiency	High	Low
Transparency	Opaque	Transparent
Color	Limited	Various
Stability	Good	Poor
Energy payback period	Longer	Shorter
Charge separation mechanism	Occurs due to the formation of an electric field in the space charge layer	Occurs due to kinetic competition (like in photosynthesis)
Light absorption and charge separation	Both functions performed by the semiconductor	Light is absorbed by dye and semiconductor solely performs charge transport

1.3 Dye-sensitized Solar Cell (DSSC) Technologies

In 1839, Becquerel found that when two platinum electrodes were dipped in the electrolyte having a metal halide salt, an electric current was produced when it is illuminated with light. After that, lighting on the organic dye was discovered in the 1960s to produce electricity in the electrical electrodes of the semiconductor cell. In the later seventies, a photoexcitation effect was first studied at the University of California to mimic the photosynthesis process by removing chlorophyll pigment from spinach and using ZnO as an electrode semiconductor material in electrochemical cells. The process was recognized by the injection of an electron into the conduction band of an n-type semiconductor scaffold material by photoexcitation of dye molecules and finding that the adsorbed dye molecules of the monolayer semiconductor were responsible for optimum yield. This research forms the basis for the biomimetic or bionic approach to sensitizing semiconductor materials to induce electrons. In 1972, Tributsch again demonstrated the production
of electricity through dye sensitization. The research by Michio Matsumura et al. in 1980 shows that by adjusting the fine porosity of the semiconductor oxide content, the efficiencies of the dye molecules may be increased, but the stabilization of the dye is a basic challenge in the dye-sensitized photocells. The development of the sensitized electrochemical PV system made of color-sensitization in semiconductor TiO2 material was then started in 1991 by Prof. Michael Grätzel who named it "dye-sensitized solar cell,". The new strategy is based on the 3 billion-year-old theory of Photosynthetic behavior in nature. They demonstrated that the PV system is modeled
on the dynamics of light absorption and electron transfer. The electron formed by chlorophyll is moved from one molecule to another before the chlorophyll reaction center is reached when sunlight falls on the chlorophyll molecules. The electron is transported from the reaction center to the molecule for energy conservation. The chlorophyll lacks one electron is being taken from the surrounding water molecule. The cyclical method is imitated for energy collection by sun rays using a synthetic dye medium. In the first attempt, the performance of DSSCs was less than 2%. In 2003, they used ruthenium-based dyes and polymer gel with good thermal stability to improve the performance of the system and achieved a maximum efficiency of approximately 6%. In 2005, scientists focused on improving the quantum performance of DSSCs, adjusting photoanode scaffolding material morphology and improving the electron transfer in the semiconductor, and developing a small-sized particle with a large surface area

to provide additional color adsorption, etc. In 2005, the ruthenium-based coloring was then replaced by low costs coloring and reached a productivity of about 5%. In 2008, the iodine-based redox fluid electrolyte produced 8% efficiency. The researchers then sought to overcome the corrosive nature of the electrolyte, thereby improving photovoltage, performance, and system stability. In this period, the efficiency of the devices increased up to 11.5%. Finally, by using porphyrin as a color loop, cobalt (II / III), and electrolyte, the performance was increased further by over 13%. Later in 2009, G24 Power Limited first marketed DSSCs, Imperial Park, South Lake Road, Newport, UK [25]–[30]

1.3.1 Working Principal of DSSC

- To provide a large surface area for adsorbing sensitizers, Nanocrystalline TiO_2 is deposited on the conducting electrode.
- Dye molecules are excited from the highest occupied molecular orbitals (HOMO) to the lowest unoccupied molecular orbital (LUMO) due to the absorption of photons.
- Once the injection of an electron into the conduction band of the wide bandgap semiconductor nanostructured TiO_2 film occurs, the dye molecule (photosensitizer) turns out to be oxidized.
- The injected electron is transferred between the TiO_2 nanoparticles before being removed and provided as electrical energy to a load.
- I^-/I_3^- redox ion-containing electrolytes are used as an electron mediator between the TiO2 photoelectrode and the counter electrode.
- The oxidized dye molecules are regenerated by accepting electrons from the I^- ion redox mediator, which is then oxidized to I_3^- (tri-iodide ions).
- The I_3^- ion replaces the internally given electron with one from the external load and reduces it back to the I^- ion.

The good thing in DSSC is that the generation of electric power causes no permanent chemical change or transformation.

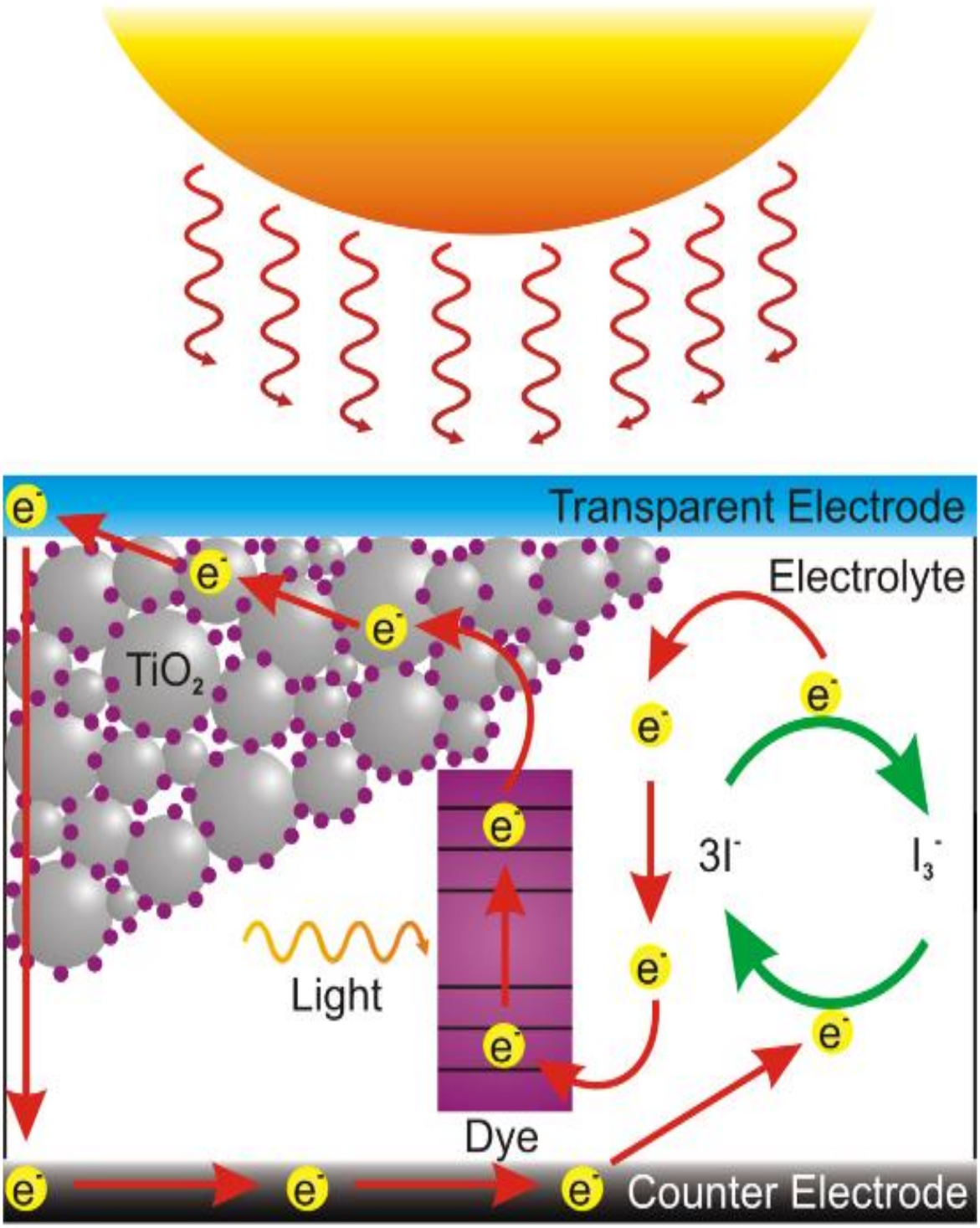

Fig. 1.3 Working principle of Dye-Sensitized Solar Cells

1.4 Advantages of DSSCs

1.4.1 Optimized performance in real-world conditions

The benefit that these solar cells have over other solar technologies is that they have the facility to tune the dye according to the conditions of electromagnetic radiation hence can be used in outdoor as well as indoor applications. These cells, not like other solar cell technologies, can perform well in real-world conditions like hazy and cloudy days, at dawn or dusk, at higher altitudes.

1.4.2 Low Embodied Energy and Technology

Another advantage of DSSCs over other technologies in solar cells is that these cells are Nano-based. One of the most important DSSC materials that form the photoelectrode of the cell is TiO2, a nanostructured semi-conducting substance. For nanostructured materials the processing temperature is much smaller, i.e., for TiO2 microparticles, the temperature is about 1000 °C and for TiO2 nanoparticles, the temperature is around 600 °C. This decreases energy consumption and reduces energy efficiency in the production of cells at low temperatures.

1.4.3 Low Manufacturing Cost

DSSCs do not require extremely pure material, as required in traditional photovoltaic technology, vacuum treatment, and strict cleanliness. Its manufacturing does not require costly equipment either. These cells can be produced in a simple environment with cheaper equipment and quick techniques such as printing and baking. Therefore, these cells have low capital costs [31].

1.4.4 Variety of Substrates

These cells can be produced on many substrates such as metal, polymer, and glass. These cells may be made on durable or versatile substrates. The illumination on both sides of the panels absorbs and transforms them.

1.4.5 Environment-friendly Materials

The materials being used in DSSCs are all non-toxic. There are no health issues involved with their production and minimum precautions should be followed during their production. Ru-based dyes are tested and found to be non-mutagenic. Some solar cells belonging to other technologies are based on very toxic materials like cadmium and selenium and they are to be handled very carefully observing many precautions.

1.4.6 Thin Film Technology Saves Resources

DSSCs involve thin films of the materials to be coated. Semiconductor coating has a thickness of just 20 μm and consists of a single layer of adsorbed pigment that is nearly 80 μm thinner than human hair. Whereas crystalline silicon cells require comparatively very thick materials and a huge amount of material during processing is wasted. Hence implementing these cells saves resources.

1.4.7 Aesthetics

For architects, it is appealing because DSSCs provide versatility in terms of clarity and coloring. Such flexibilities are not offered by any other solar cell technology. Because of the clear and infinite choices of shades, the architects use these cells as doors, screens, inner walls, and skylights. Doors and windows based on DSSC can produce power, provide noise and heat insulation, and reduce the strength of harsh sunlight. Color choices can be offered with red, black, green, orange, grey, yellow, and brown coloring that can attract the eye.

1.4.8 Readily Available Raw Material

Titanium/Zinc, hydrogen, oxygen, silicon/iron, and carbon are the most used chemical materials in DSSCs which are readily available and comparatively cheap. Platinum and ruthenium are also key ingredients in these solar cells but they are required in very small amounts.

1.4.9 High-temperature Performance

The efficiency of DSSC does not degrade with increased temperature, meaning you can continue to efficiently harvest energy in direct sunlight.[31][32][33][34][35].

1.5 Applications of DSSCs

DSSCs have many applications few of which are stated below:

- DSSCs modules are used to generate electricity. They can be particularly used in remote areas where grid electricity is not available
- Individual cells may be used to power small devices like wristwatches, calculators, etc.
- They can have their applications in Remote sensors, Building management (Motes), Mobile communications, Sonobuoys, and remote transmitters.

Chapter 2

LITERATURE REVIEW

Dye-sensitized solar cells (DSSCs), which deliver high-performance capacity and significantly lower production costs concerning conventional silicon-based solar power, are among the most promising technology. Till now, substantial developments have been attained in terms of both optimizations of constituents and knowledge about the crucial processes that govern cell proficiency. In DSSC devices, a dye sensitizer is inserting the photo-excited electrons into the complex of unfilled states of the semiconductor, adsorbed in a mesoporous oxide film comprising of nanometer particles, generally specified as a "conduction band" (CB). The reestablishment of the dye's ground state is due to the contribution of an electron from an electrolyte to the oxidized dye at the counter electrode retaining the reduction method, it regenerates the dye molecules and ends the electrical circuit.

The general enactment of the DSSC is intensely focused on the effectiveness of the forward transfer of electrons and the charge transference process which are in turn depending on the photo-electrochemical and structural characteristics of the dye sensitizer, among others. Probably strongly combined with the oxide conduction band states, a high-efficient sensitizer must have a extensive range of adsorption in the ultraviolet (UV) and nuclear infra-red (NIR) spectrum that is related to long-term charge separation of the excited state. Several metal-free dyes and Ru(II) based dyes permitting the preparation of simpler and low-rate DSSC based on I^-/I_3^- electrolyte, that approach the proficiency up to 10%. Recently, organic dyes have attained an impressive 13% of efficiency with metal porphyrins in combination with a cobalt electrolyte.

The limited performance of organic sensitizers was due to both charge recombination of inserted electrons with the oxidized dye or electrolyte and to the founding of dye masses at TiO_2 surface, considering their typically large extermination coefficients. The inserted electrons recombination with oxidized dyes follows a non-adiabatic mechanism that relies on the density of electrons in the semiconductor conduction band states, electrolyte composition as well as on the three-dimensional separation of the highest occupied molecular orbital (HOMO) of the dye and the surface of TiO_2. The kinetics of this technique of recombination directly affect the charge density through the semiconductor, and therefore, the open-circuit voltage of the cell, V_{oc}, which differs from the quasi-Fermi level of the semi-conductor under illumination to the electrolyte redox potential. The flow of the injected electrons in an open

circuit is equal to that of the recombination electrons, which fixes the Fermi level and therefore the output voltage of the device. The determination of Fermi-level is due to the conduction band edge potential and by the electron density into the TiO_2, which is proportional to the rate of the electron injection and the lifetime of an electron, τ [36].

2.1 Effect of Structural Modification on light-capturing

This structural alteration also boosts the light-capturing capacity for electron capture and injection, making it superbly efficient for photoelectric conversion (PCE).

Recently, numerous experimental and computational studies have been fixated on the interactions between the oxidized dye and iodide and their suggestions in the dye regeneration mechanism. Some authors proposed the idea that particular atoms or chemical groups can also deliver strong binding sites for I_2 (I_3^-), increasing its concentration close to the TiO_2 surface and hence accelerate the recombination methods by keeping the reduced electrolyte far from the direct contact with oxide surface.

Elshafie A.M. Gad *et.al* **experimentally** tested 6,7-dihydroxy-8-[(E)-(4-methoxyphenyl) diazenyl]-4-methyl-2Hchromen-2-one, (D1) 6,7-dihydroxy-8-[(E)-(4-hydroxyphenyl) diazenyl]-4-methyl-2H-chromen-2-one (D2), and 6,7-dihydroxy-4-methyl-8-[(E)-(4-methylphenyl) diazenyl]-2H-chromen-2-one (D3) as photosensitizer in solar cell and conducted a **computational** study in a photovoltaics cell to explain the proficiency of these complexes as photo-sensitizer

Density functional theory (DFT) studies were carried out to find the polarizability (<α>), the anisotropy of the polarizability (<Δα>), ground-state dipole moment (μ) and the first-order hyperpolarizability (β) of the dyes using Gaussian 09 and Gauss View v.6.0 established on keywords: ‘‘optimized frequency b3lyp/6-311G++ (d, p) guess = mix pop = (nbo, savenbos) geom = connectivity polar = opt rot. They also inspected the E_{HOMO} (Highest occupied molecular orbital energy), E_{LUMO} (Lowest unoccupied molecular orbital energy), HOMO-LUMO energy gap (ΔE), electron affinity (A), and ionization potential.

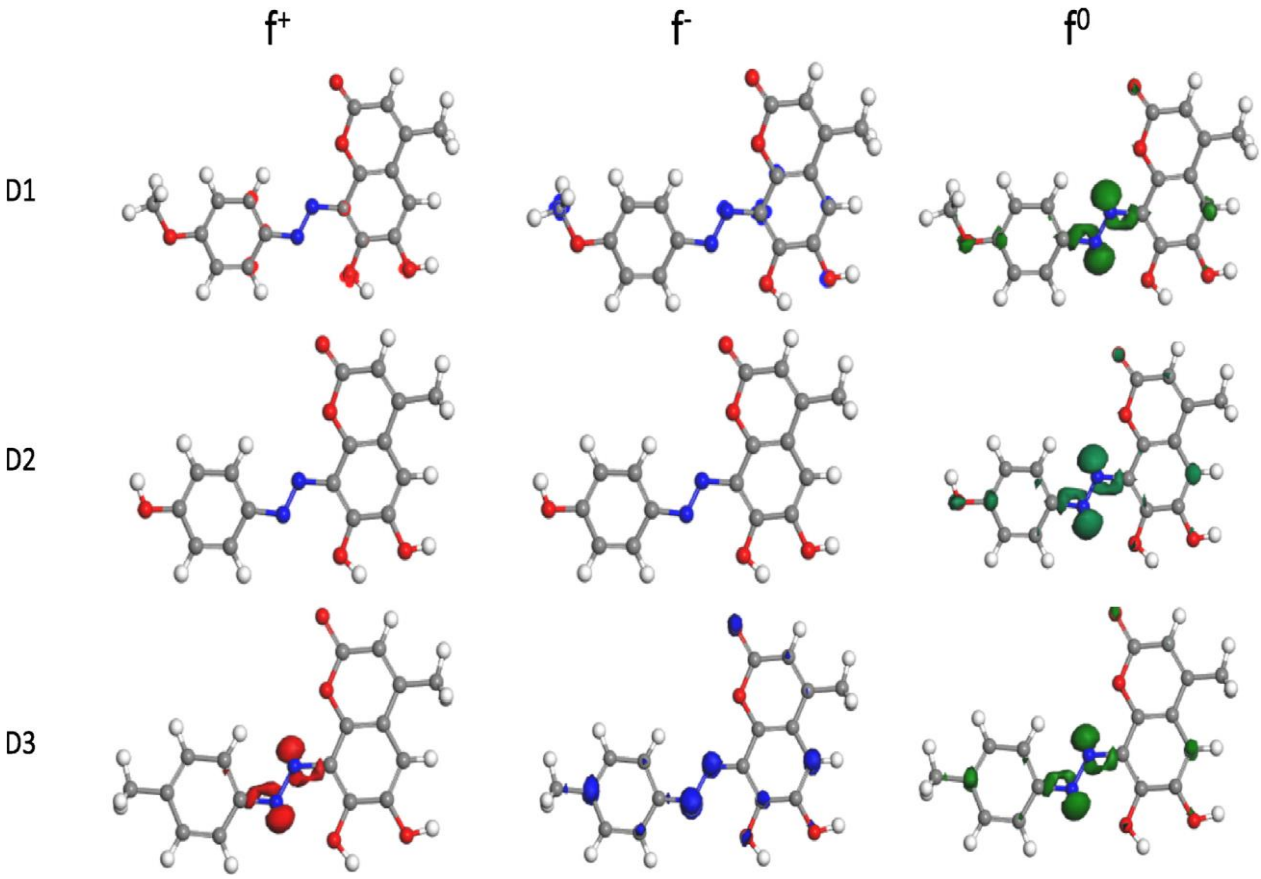

Fig 2.1: Graphical representation of investigated dyes.

Their calculation was established on the structure variation of the dyes with electron-withdrawing groups (HO-C and CH_3-O-C) and electron repelling group (H3C-C) based on a push-pull framework of Qumarin was studied. The enhancement of qumarin based dyes can diminish the energy gap and produce a redshift as per the simulation suggestion [37].

Chaofan Sun *et.al*, experimentally investigated the photoelectrical properties of two dyes, ethyl red, and carminic acid, as sensitizers of dye-sensitized solar cells. Density functional theory (DFT) and time-dependent density functional theory (TDDFT) studies were carried out to calculate the ground and excited-state properties of the dyes before and after the adsorption on TiO_2, to reveal the reason for the difference between the photo-electrical properties of the two dyes. The investigated parameters are the light-harvesting efficiency (LHE), the dynamic force of electron injection (ΔG^{inject}) and dye regeneration (ΔG^{regen}), the total dipole moment (μ^{normal}), the conduction band of the edge of the semiconductor (ΔE^{CB}), and the excited-state lifetime (τ) that are narrowly correlated to the short-circuit current density (J_{sc}) and open-circuit voltage (V_{oc}).

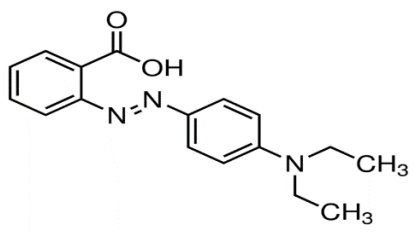

Ethyl red (a)

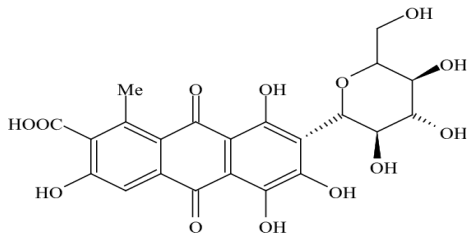

Carminic Acid (b)

Fig 2.2: Chemical structures of (a) Ethyl red and (b) Carminic Acid

They originate that the experimental carminic acid has a larger Jsc and Voc, which are understood by a larger amount of dye adsorbed on a TiO_2 photoanode and a larger ΔG^{regen}, excited-state lifetime (τ), μ^{normal}, and ΔE^{CB}. At the same time, chemical reactivity constraints elucidate that the lower chemical hardness (h) and higher electron-accepting power (ω^{+}) of carminic acid influence the short-circuit current density. Hence, carminic acid shows superb photoelectric conversion efficiency in association with ethyl red [38].

M. Hachi *et.al*, designed the four donor-π-acceptor dyes based on benzo carbazole as a donor by varying the bridge groups. The evaluation of their optoelectronic and photovoltaic properties occurred using density functional theory (DFT) and time-dependent DFT (TDDFT) methods. Several key parameters were examined to detect the impact of Spacer group modulation to improve light absorbance capability and increase intramolecular charge transfer.

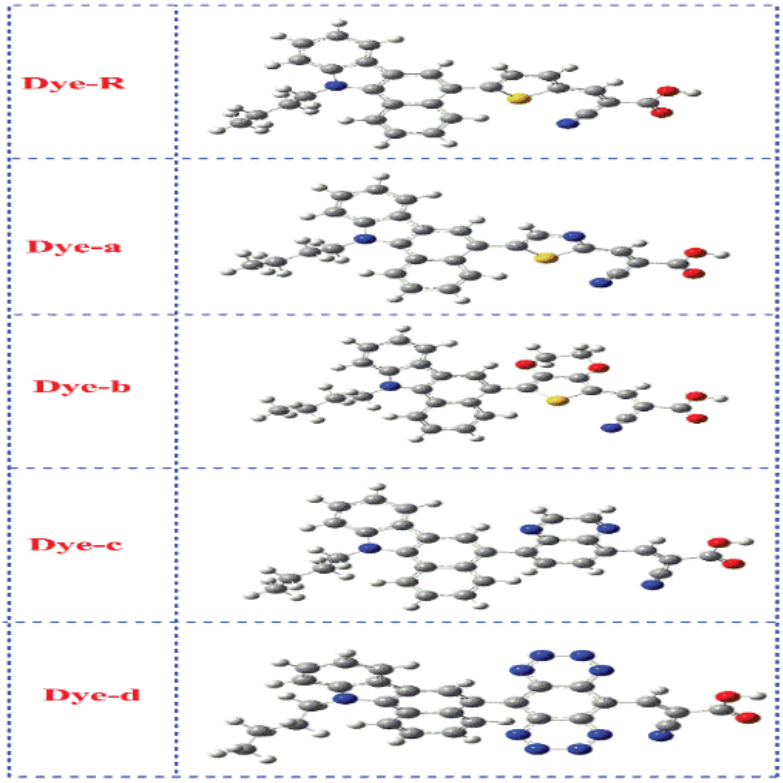

Fig 2.3: Optimized Structure of studied dyes obtained by B3LYP/6-31G(d,p) level.

It indicates the molecule Dye-c shows the best performance among the designed dyes from the result, showing low-lying HOMO energy level (-5.29eV), small energy gap (2.47 eV), a maximum wavelength of 446nm. This contribution can be an important guide for the production of effective DA dyes for dye-sensitive solar cells (DSSCs) [39].

Jesús Baldenebro-López *et.al*, reported a copper complex-based dye, which is proposed for potential photovoltaic applications and is named Cu (I) biquinoline dye. Based on the density functional theory (DFT) and time-dependent DFT (TDDFT), they used results of electron affinities and ionization potentials for the correlation between different levels of calculations used in their studies. Further, they compared the maximum absorption wavelengths of their theoretical calculations were compared with the experimental data. They found that the M06/LANL2DZ + DZVP level of calculation provides the best approximation. To find the optimized molecular structure and to predict the main molecular vibrations, the molecular orbitals energies, dipole moment, isotropic polarizability, and the chemical reactivity parameters that arise from conceptual DFT, this level of calculation was used [40].

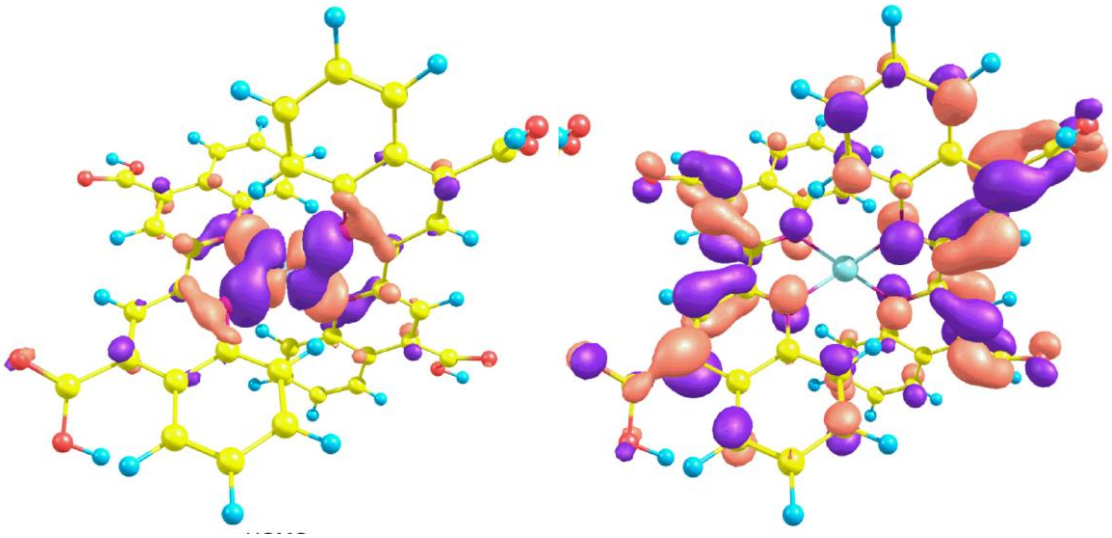

HOMO LUMO

Fig 2.4: Highest occupied molecular orbitals (HOMO) and lowest unoccupied molecular orbitals (LUMO) orbitals of Cu biquinoline dye with M06/LANL2DZ + DZVP level of calculation.

Simona Fantacci *et.al*, presented a combined Density Functional/ Time-Dependent Density Functional study of the molecular structure, electronic states, and optical absorption spectrum of [Ru(4,4'-COOH-2,2'-bpy)$_2$(NCS)$_2$], which is an extensively used charge-transfer sensitizer in dye-sensitized solar cell (DSSC). A continuum model for solvent-solution interfaces was used to calculate the complex in a vacuum and ethanol and water solvents. The insertion of the solvent convinces major energy shifts and the structure of the complex's molecular orbitals is subsequently in fair accordance with the experiment, while the computed spectrum of the Ru complex vacuum varies from the experimental spectrum in terms of both energy and shape, In the existence of the solvent the measured spectrum is in strong accordance with the experiment. Rather than pure metal-ligand charge transfer (MLCT) transitions, the first two absorption bands were found to initiate from mixed ruthenium-NCS to bipyridine-π^* transitions, while the third band arises from intraligand π-π^* transitions. The experimentally observed blue shift in the spectrum of ethanol in water is well reproduced in our calculations and seems to have a relation with a diminished dipole moment in the excited state [41].

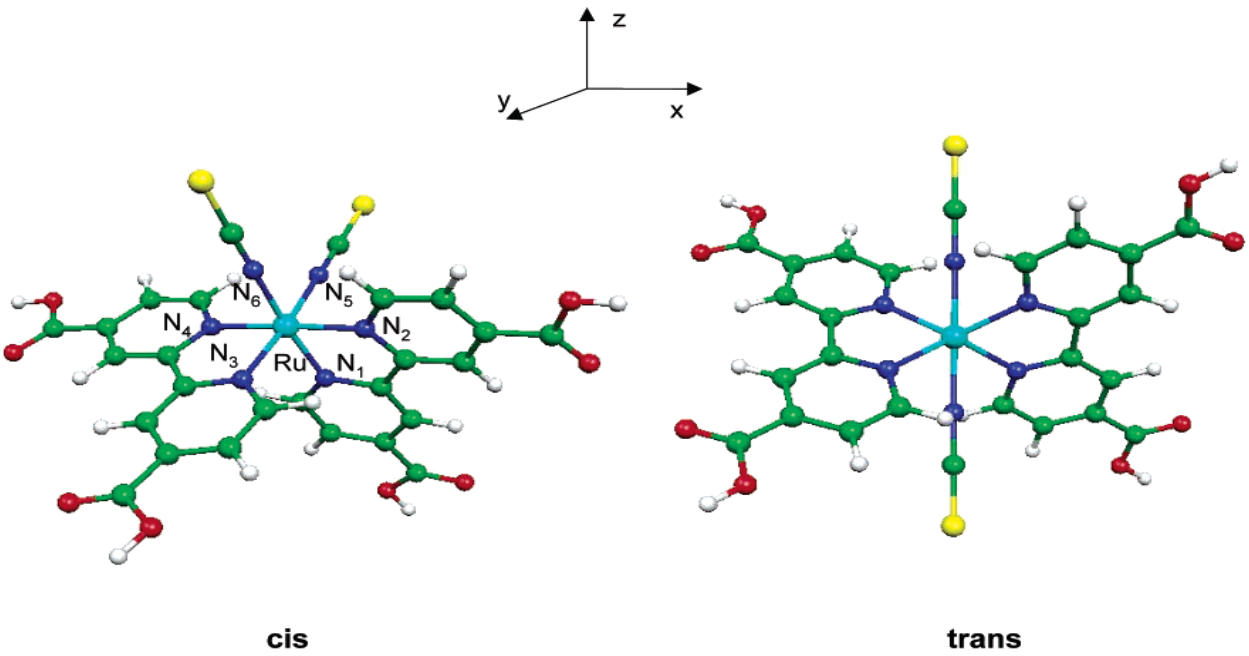

Fig 2.5: Optimized structure of the cis and trans isomers of the [Ru(4,4¢-COOH-2,2¢-bpy)2(NCS)2] complex

2.2 Gap Identification

Modern researchers investigated several materials for the adsorption of dyes in organic dye-sensitized solar cells experimentally and computationally. Some preliminary computational studies were also performed to analyze the interaction of dye adsorption with nano-particles, and also introducing different types of electrolytes. The current work is related to develop and study the performance of a new generation of organic dyes for dye-sensitized solar cells. In association with computational and organic chemists, new organic molecules were designed and studied as sensitizers in the solar cell. Overall device performance of DSSC is governed by the adsorption, electron injection, and charge collection efficiencies. The vital role of the sensitizing dye is to harvest as much visible light as possible. To increase light-harvesting of organic dyes, their adsorption should be personalized to match with the high photon-flux region of solar radiation. The D-π-A type design is one of the promising strategies to achieve a desirable adsorption region. To improve the electron-injection efficiency, the anchoring unit of an all-organic dye should be able to undergo strong electronic coupling with the semiconducting oxide electrode. The current study focused to explore a better understanding of the adsorption behavior of organic dyes [44]. In the adsorption studies, distance plays an essential role and has contributed substantially to adsorption constant, free energy, enthalpy, and adsorption energy. Frontier orbital interactions between dyes, Nano-crystalline TiO_2, and electrolytes also helped us to predict the extent of orbital overlap adsorption behavior. Potential energy surfaces (PES) also inferred the stability and binding property between adsorbate and adsorbents.

On the other hand, the behavior of the novel dyes incorporated in the DSSC showed less predictive photovoltaic results. This project was designed to find the limiting role of dye energy without compromising the action of the essential processes of electron transfer concerning the dye. The core of this study is the identification of processes and characteristics that restrict DSSC system efficiency.

2.3 Problem Statement

The low efficiency of Dye-Sensitized Solar cells (DSSC) is attributed to the barrier of electron transfer from dye excited state to TiO2. Inorganic dyes being used in DSSC tend to agglomerate due to reduction by I_3^- leading to poor functioning of DSSC. Due to the large number of functional groups available for molecular design, there is still much work for DSSC performance improvement.

2.4 Solution Statement

Nano-particles are currently widely used for adsorption in the modern age. Many researchers adsorb various dyes on the surface of adsorbents in dye-sensitized solar cells, but very few theoretical studies have been published to examine the computational adsorption activity of coumarin-dyes hybrids. The current work is based on the designing of a metal-free organic dye sensitizer for a dye-sensitized solar cell with donor-π-acceptor (D-π-A). The photophysical intramolecular charge transfer characteristics of D-π-A can be changed by making appropriate dye substitutions. In this project, we will design a hybrid of a carbazole-coumarin contributing model of D-π-A for efficient electron transfer.

Table 2.1: The names and structures of all the five coumarins and a carbazole are shown in the table:

IUPAC Names	Abbreviations	Structures
6,8-Dimethoxy-7-methyl-3-phenylisocoumarin	Coum-1	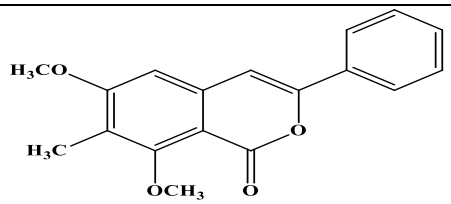
6,8-Dimethoxy-7-methyl-3-(p-tolyl)isocoumarin	Coum-2	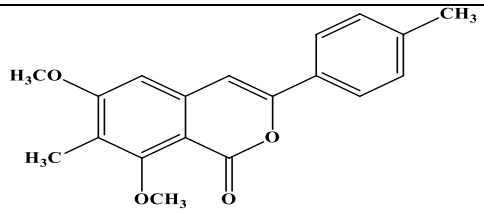
6,8-Dimethoxy-7-methyl-3-(4'-methoxyphenyl)isocoumarin	Coum-3	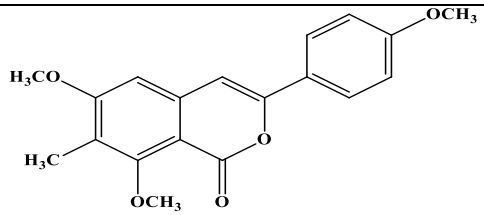
6, 8-Dimethoxy-7-methyl-3-(4'-chlorophenyl) isocoumarin	Coum-4	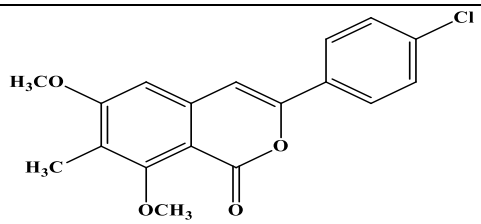
6, 8-Dimethoxy-7-methyl-3-(4'-nitrophenyl) isocoumarin	Coum-5	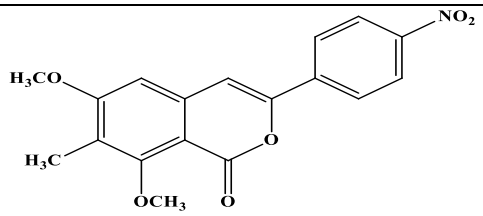
3,5-dinitro-N-octylcarbazole	Carbazole	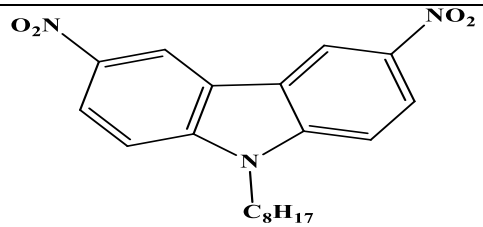

2.5 Chemical Structures of Coumarin-Carbazole Hybrids

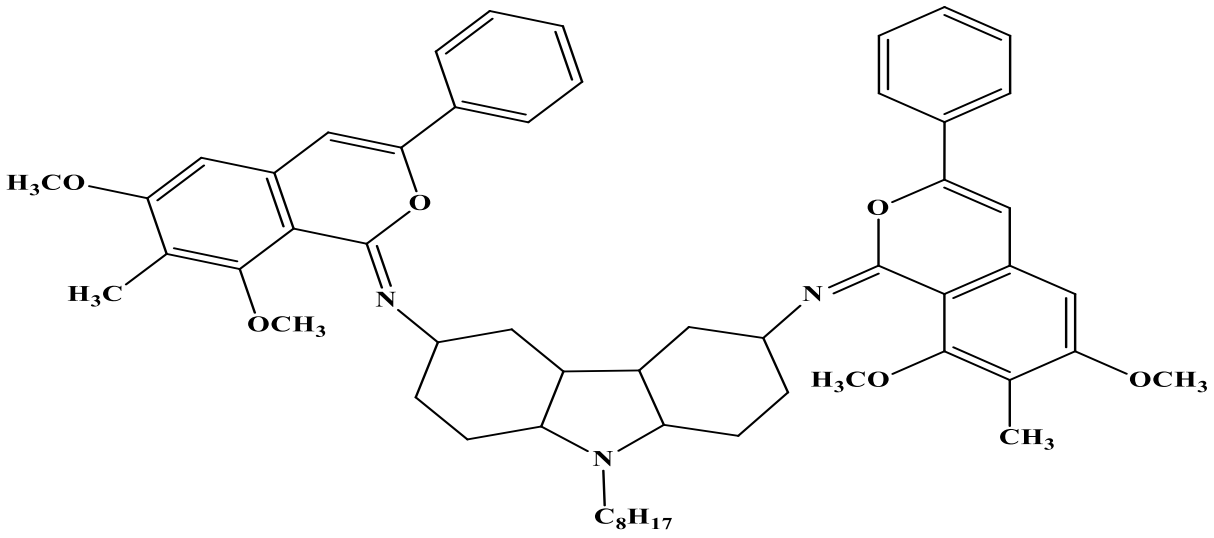

Fig 2.6: Chemical structure of coumarin 1-carbazole Hybrid (HK-1)

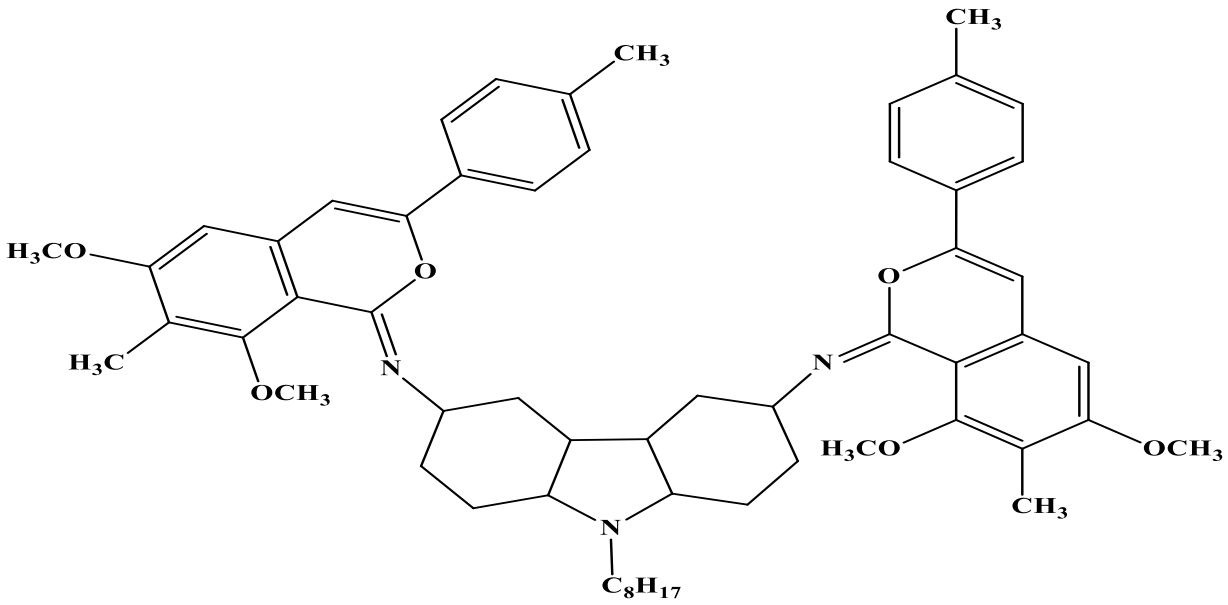

Fig 2.7: Chemical structure of coumarin 2-carbazole Hybrid (HK-2)

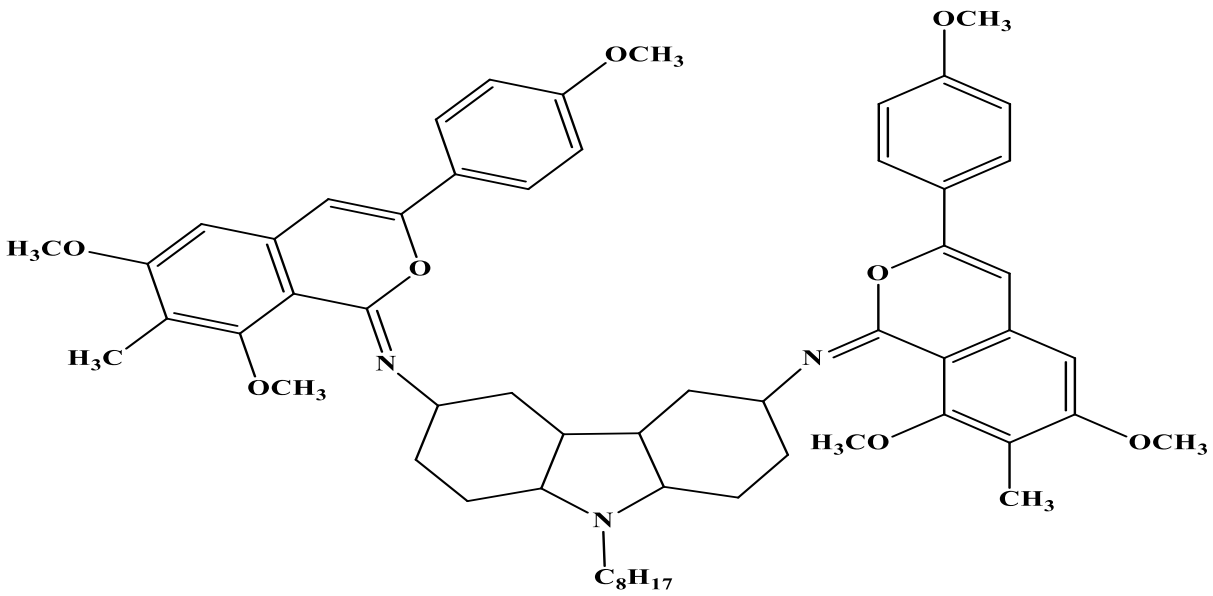

Fig 2.8: Chemical structure of coumarin 3-carbazole Hybrid (HK-3)

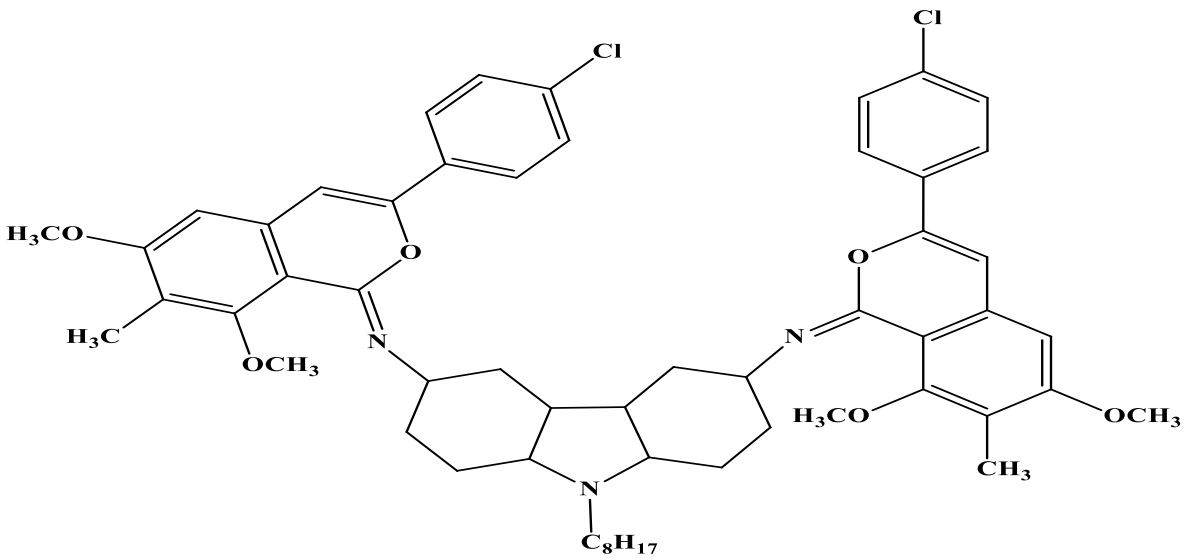

Fig 2.9: Chemical structure of coumarin 4-carbazole Hybrid (HK-4)

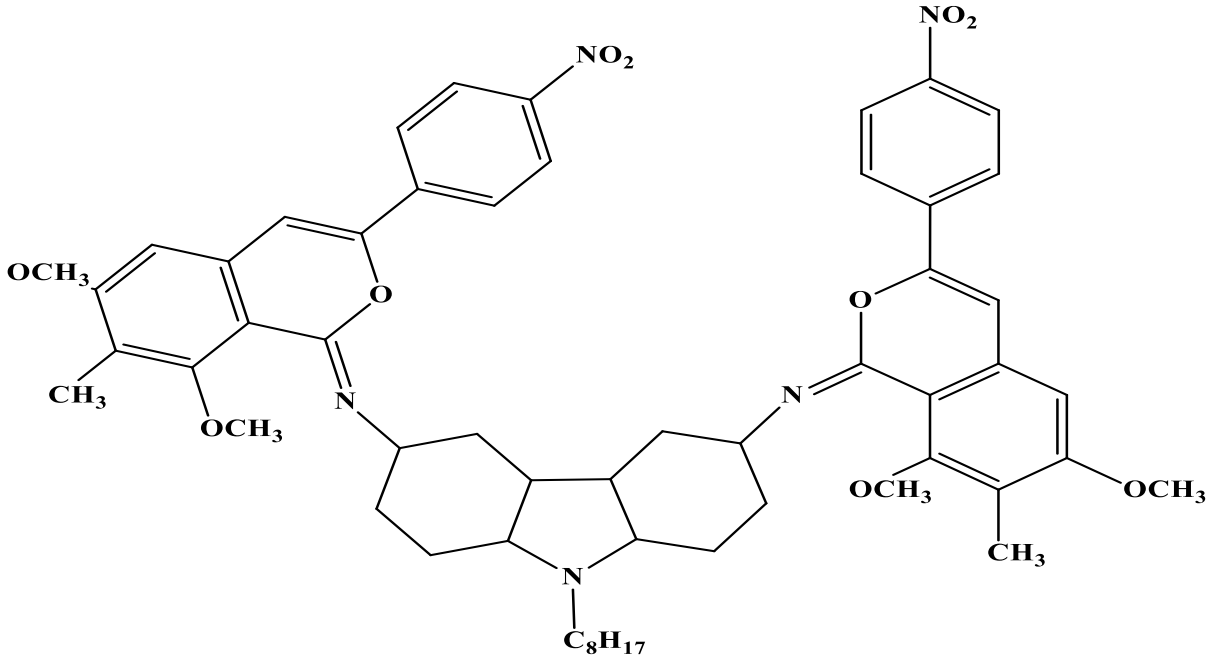

Fig 2.10: Chemical structure of coumarin 5-carbazole Hybrid (HK-5)

2.6 Objectives

The main objectives of the current project are as follow:

- To model the dye-iodide interactions in organic solar cells.
- To determine the interaction between the dye and Ti^{3+} cation as well as the formation of Dye- I_3^- complexes.
- To find the preferred binding site of oxygen atoms for I_2 and the interaction of I_3^- with the π system of the carbazole donor unit.

Chapter 3

METHODOLOGY

Chapter 3

Methodology

Computational chemistry is an interdisciplinary discipline that uses computer science to create codes and applications that can solve problems in a chemical way, often known as molecular modeling or molecular simulation. The results of theoretical chemistry are applied by these computer codes. Theoretical chemistry is, thus, the basic theory on which computational chemistry is based. Theoretical chemistry itself incorporates statistical techniques with basic laws of physics to atomically formulate the behavior of matter.

The current work is focused to explore the adsorption approach of the three hybrids of coumarin and carbazole over TiO_2 Anatase slab using density functional theory (DFT). Quantum mechanics give us all the data related to electronic structure and the corresponding properties of a molecule that can be directly derived from wave function which is obtained by solving the time-independent Schrodinger Wave equation for a multinuclear and multi-electron system.

$$H\psi = E\psi$$

where'Ψ' is the many electrons wave function, 'E' is the eigenvalue of the operator and 'H' is the Hamiltonian operator.

3.1 Computational Modeling Suite

Presently SCM Amsterdam Density Functional Modeling Suite 2019 has been employed as a powerful tool for heterogeneous adsorption of three novel dyes on the surface of monocrystalline TiO_2. Some important features of ADF 2019 modeling include:

- ADF is strong in understanding and predicting the structure, reactivity, and spectra of molecules.
- ADF offers unique aptitudes to calculate the molecular properties of nanoparticles and organic electronic materials.

- DFT calculations are easily prepared and analyzed with an integrated graphical user interface (GUI).
- ADF has modern correlation (XC) functional and all types of basis sets.

3.2 Exchange Correlation Functional

The exchange-correlation functional is the central notion of the Density Functional Theory (DFT), an approach to quantum-chemical calculations very popular recently for its competitive speed and accuracy. While the existence of the universal functional has been proved, its exact formulation remains unknown. This leads to a proliferation of approximations, each having specific strong and weak points. The structure of DFT calculations requires several derivatives of the function to be.

3.3 Density Functional Theory (DFT)

Density functional theory (DFT) is a computational quantum-mechanical approach for simulating the electronic structure of many-body systems, especially atoms, molecules, and condensed phases, utilized in physics, chemistry, and materials science.

At first, input structures of all the five coumarins dyes, a carbazole, and their hybrids were created on ADF Modelling Suite 2019, performed geometry optimization using a basis set of GGA-LDA PBE-G. Through optimization, we calculated the adsorption energy (E_a), frontier molecular orbital E_{HOMO}-E_{LUMO} gaps, and infrared spectrum. Then we generate a slab of titanium dioxide TiO_2 and performed optimization and then adsorbed all the five coumarin dyes, a carbazole, and their five hybrids over TiO_2 and calculated their energies in terms of fragment energy.

3.4 Performed Objectives of Methodology

Objectives of the present research work are performed by using exchange-correlation and DFT as described below:

Objective-1

At first, we modeled the five **coumarins** and a **single carbazole dye** on **ADF 2019**. Then we perform geometry optimization using a basis set **GGA-PBE**. Then we modeled the **hybrids** of **coumarin** and **carbazole** and also performed optimization using the same basis set to obtain the **frontier orbital calculations**, in which we found $\mathbf{E_{ox}}$ (Oxidation energy), $\mathbf{E_{red}}$ (Reduction energy), and **Excited-state oxidation energy ($\mathbf{E_{ox*}}$)** for **coumarins** and **hybrids** individually.

Objective-2

In the second objective, we generated a slab of titanium dioxide TiO_2 on the ADF 2019 Band that is Anatase, a space group of TiO_2. Then we performed periodic multilayer slab generation optimization using a basis set of **GGA-D-PBE-D**, in which we found the Density of States (DOS) of TiO_2. Through DOS, we found the value of the conduction band, based on which we obtained the efficiency of DSSC.

Objective-3

In the third objective, firstly we adsorbed the five coumarins and a single carbazole dye on the TiO_2 Anatase surface using periodic DFT calculations having the basis set of **GGA-PBE**, then we adsorbed hybrids of coumarin and carbazole on TiO_2 using the same calculations and basis set. In this objective, we calculated the adsorption energies for both the coumarins and hybrids individually and also $\mathbf{E_{ox}}$ (Oxidation energy), $\mathbf{E_{red}}$ (Reduction energy), and $\mathbf{E_{ox*}}$ (Excited-state oxidation energy).

Chapter 4

Results & Discussions

Presently, the interaction of five coumarins **6,8-Dimethoxy-7-methyl-3-phenylisocoumarin, 6,8-Dimethoxy-7-methyl-3-(*p*-tolyl)isocoumarin, 6,8-Dimethoxy-7-methyl-3-(4'-methoxyphenyl) isocoumarin, 6,8-Dimethoxy-7-methyl-3-(4'-chlorophenyl) isocoumarin, and 6,8-Dimethoxy-7-methyl-3-(4'-nitrophenyl) isocoumarin** with carbazole **(3,5-dinitro-N-octylcarbazole)** are studied for adsorption on TiO_2 anatase surface employing the computational DFT method for dye-sensitized solar cell applications. In comparison to coumarin and carbazole, plane-wave calculations demonstrate that the hybrids have a relatively strong binding to the TiO_2 surface. The density of states (DOS) was generated to monitor the overlap of the hybrids' molecular orbitals and the TiO_2 band. Oxidation potentials of five coumarins, carbazol, and their hybrids were determined to evaluate electron injection from hybrids to TiO_2 slab through adsorption mechanism.

The feasibility of adsorption was estimated through the energy of adsorption by using the following equation:

$$\Delta E_{ads} = E(A\text{-}B) - (E_A + E_B)$$

Whereas E_A is the energy of adsorbent A (anatase TiO_2 here), E_B is the energy of the adsorbate B(coumarin, carbazole, and their hybrids here) and E(A-B) is the energy of the complex formed after adsorption of A on B. To build up a better comprehension of adsorption measures, we have hypothetically researched parametric assessment of adsorption constant (K_D) and frontier molecular orbitals calculations (E_{LUMO} and E_{HOMO}) after the adsorption of each coumarin and carbazole decided the immediacy of reaction and strength of hybrid between carbazole and coumarin dyes.

***Table 4.1**: Energetic parameters for adsorption of Coumarin on the surface of Titanium dioxide (TiO_2) calculated at LDA-GGA (Local density approximation – Generalized gradient approximation) level theory.*

No.	**ΔE_{ads} = $E_{Coum\text{-}TiO2}$ – (E_{Coum} + E_{TiO2})**				**Complex – (Coum + TiO_2)**
	Coum-TiO_2 Bond E eV	Coum Bond E eV	TiO_2 Bond E eV	Coum +TiO_2 Bond E eV	ΔE_{ads} eV
Coum-1	-6.658×10^3	-235.3668	-7.8816	-243.2484	-6.415×10^3
Coum-2	-6.809×10^3	-250.4626	-7.8816	-258.3442	-6.551×10^3
Coum-3	-7.034×10^3	-255.4039	-7.8816	-263.2855	-6.770×10^3
Coum-4	-7.367×10^3	-231.0994	-7.8816	-238.981	-7.128×10^3
Coum-5	-7.239×10^3	-245.6957	-7.8816	-253.5773	-6.977×10^3
Carbazole	-7.515×10^3	-170.329	-7.8816	-178.2106	-7.337×10^3

Five novel coumarin dyes have been optimized utilizing DFT studies names are shown in Table: 4.1. After optimization, we observed that all five coumarin dyes have negative energy values, which shows that all five coumarin dyes show physisorption behavior. Coum-4 has a higher negative value, so it has been adsorbed most efficiently as compared with the other four coumarin dyes due to the higher donor group chlorine in its structure. Coum-1 has the least negative value as compared with the other four coumarins due to the highest accepting group i.e., $-OCH_3$.

***Table 4.2**: Energetic parameters for adsorption of Coumarin-carbazole hybrids on the surface of Titanium dioxide (TiO_2) calculated at LDA-GGA (Local density approximation – Generalized gradient approximation) level theory.*

	ΔE_{ads} = $E_{Hybrid\text{-}TiO2}$ – (E_{Hybrid} + E_{TiO2})				**Complex – (Hybrid +TiO_2)**
No.	Hybrid-TiO_2 Bond E eV	Hybrid Bond E eV	TiO_2 Bond E eV	Hybrid +TiO_2 Bond E eV	ΔE_{ads} eV
HK-1	-1.3130×10^4	-730.8967	-7.8816	-738.7783	-1.2391×10^4
HK-2	-1.3433×10^4	-758.7849	-7.8816	-766.6665	-1.2666×10^4
HK-3	-1.3887×10^4	-715.8411	-7.8816	-723.7227	-1.3164×10^4
HK-4	-1.4641×10^4	-576.8352	-7.8816	-584.7168	-1.4057×10^4
HK-5	-1.4367×10^4	-359.7634	-7.8816	-367.645	-1.4×10^4

Five novel hybrid dyes have been optimized utilizing DFT studies names are shown in Table: 4.2. After optimization, we observed that all five hybrid dyes have negative energy values, which shows that all five hybrid dyes show physisorption behavior. HK-4 has a higher negative value, so it has been adsorbed most efficiently as compared with the other four hybrid dyes due to the higher donor group chlorine in its structure. HK-1 has the least negative value as compared with the other four hybrids due to the highest accepting group i.e., $-OCH_3$.

4.1 Adsorption of C1 – C5 on TiO_2 anatase (101) surface

Density functional theory (DFT) calculations were used for a model structure (MS) to investigate the anchoring behavior of these dyes on the TiO_2 anatase (101) surface because structural variation is mainly enforced on the isocoumarin moiety for all of these molecules. To lessen the computational cost, the benzene ring has been substituted in MS with four additional substituents: methyl, methoxy, chlorine, and nitro groups. The anatase surface model was employed in the current calculations of a periodically repetitive slab to explore the many credible adsorption configurations of MS on the metal oxide surface.

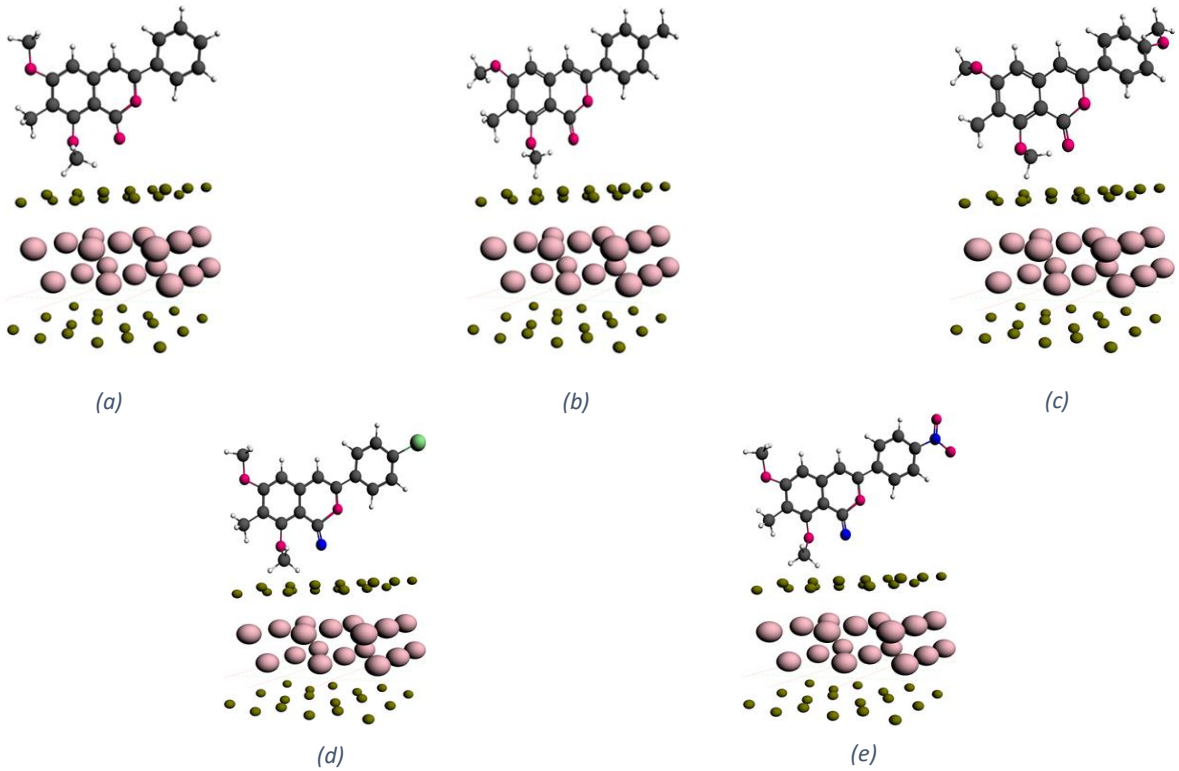

Fig 4.1: Optimized TiO_2 slab and optimized structures of coumarin dyes on TiO_2 anatase (101) surface.

4.2 Adsorption of Hybrids on TiO2 anatase (101) surface

Density functional theory (DFT) calculations were used for a model structure (MS) to investigate the anchoring behavior of these dyes on the TiO_2 anatase (101) surface because structural variation is mainly enforced on the isocoumarin making hybrid with carbazole for all of these molecules. To diminish the computational cost, the isocoumarin combines with carbazole in MS with four additional substituents: methyl, methoxy, chlorine, and nitro groups to form a hybrid. The anatase surface model was employed in the current calculations of a sporadically recurring slab to investigate the many probable adsorption conformations of MS on the metal oxide surface.

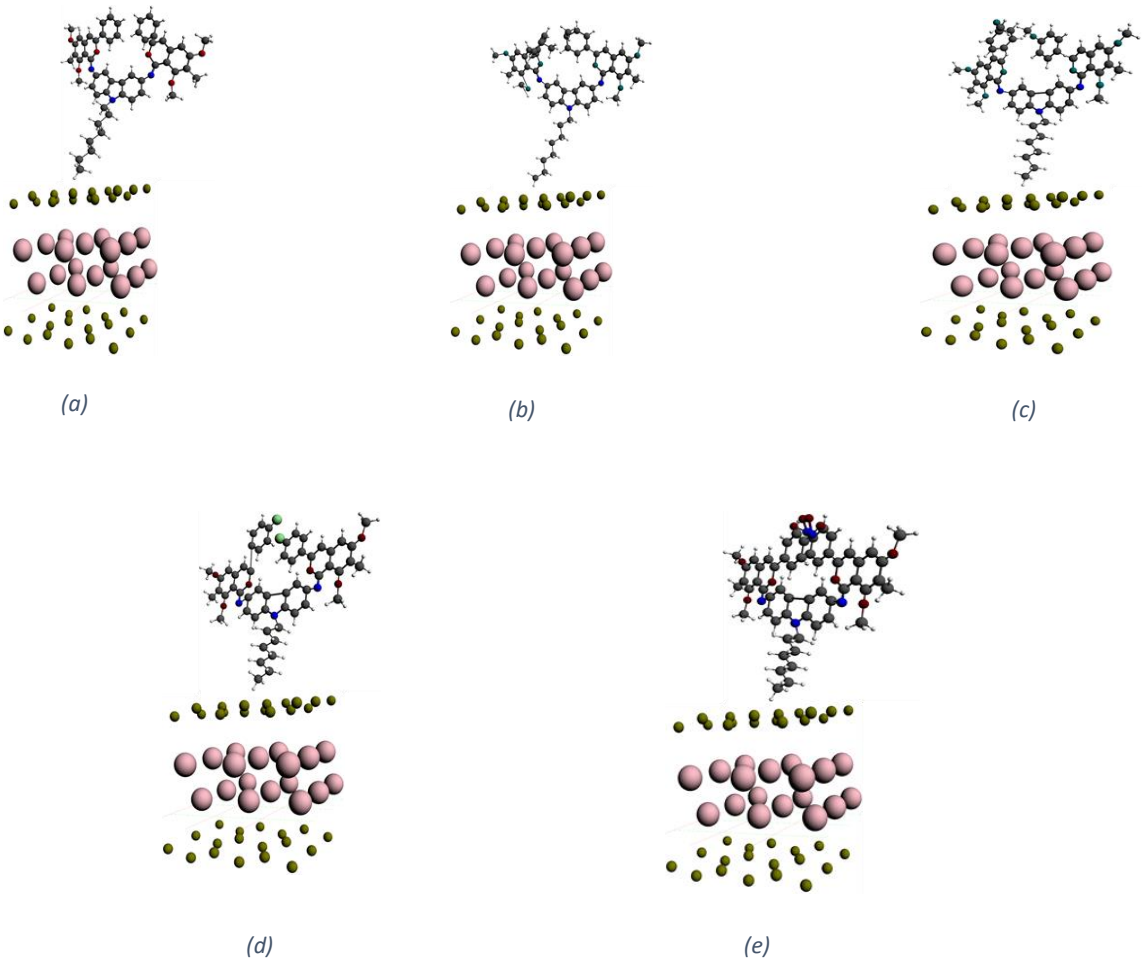

Fig 4.2: Optimized TiO_2 slab and optimized structures of hybrid dyes on TiO_2 anatase (101) surface.

4.3 Molecular orbital analysis of Coumarin dyes

The molecular orbital analysis of the frontier orbitals of all the coumarin dyes has been carried out using DFT studies obtained at the GGE-PBE-D level of theory, to validate the thermodynamic probability of electron injection from the excited state of the dye to the conduction band of TiO_2. The electronic scattering for the HOMO and LUMO of the five coumarin dyes is portrayed in Fig. 4.3. The HOMO of these compounds is localized on both the dyes and the TiO_2, while the LUMO is also localized on both the dyes and TiO_2. All these dyes endure a physisorption reaction. The charge transfer excitation could be unproductive due to the electronic dissemination over both in HOMO and LUMO, through this planar bridge. The transition between these two (HOMO – LUMO) can be deliberated as a charge transfer excitation and the levels of HOMO and LUMO are well alienated for the electronic distribution, but the transfer of an electron could not be easily done from LUMO to TiO_2 in coumarin dyes.

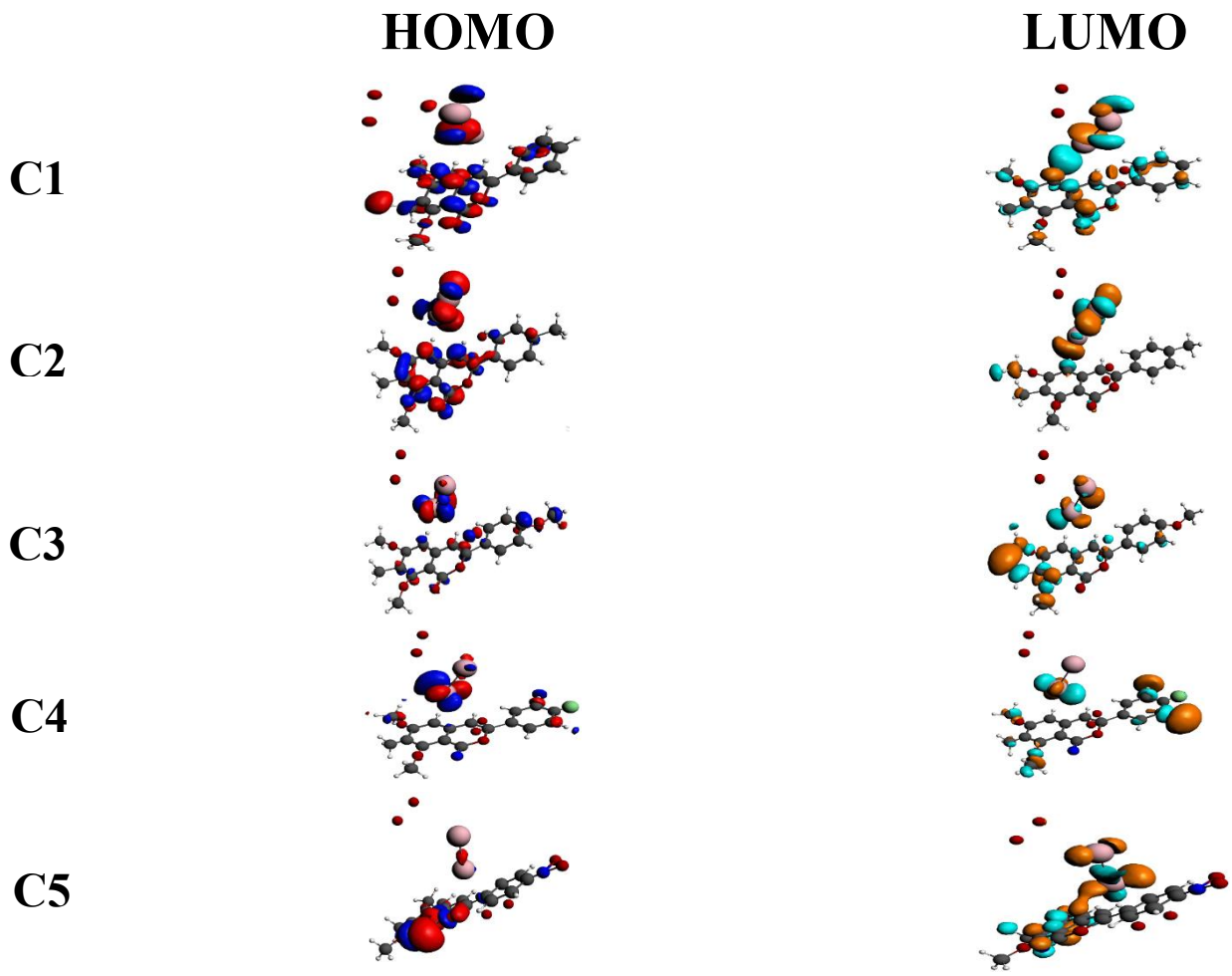

Fig 4.3: Computed isodensity surfaces of the HOMO and LUMO of the Coumarin dyes.

4.4 Molecular orbital analysis of Coumarin – Carbazole hybrid dyes

The molecular orbital analysis of the frontier orbitals of all the coumarin- carbazole hybrid dyes has been carried out using DFT studies obtained at the GGE-PBE-D level of theory, to validate the thermodynamic possibility of electron injection from the excited state of the dye to the conduction band of TiO_2. The electronic dissemination for the HOMO and LUMO of the five hybrid dyes is portrayed in Fig. 4.4. The HOMO and LUMO of these compounds are confined on the dyes, except HK-2. Due to the methoxy group, which is electron-donating in nature, the HOMO and LUMO are localized on both the dyes and TiO_2. All these dyes undergo a physisorption reaction. The charge transfer excitation could be effective due to the electronic distribution over both in HOMO and LUMO, through this planar bridge. The transition between these two (HOMO – LUMO) can be considered as a charge transfer excitation and the levels of HOMO and LUMO are well separated for the electronic distribution, and the transfer of an electron could be easily done from LUMO to TiO_2 in hybrid dyes.

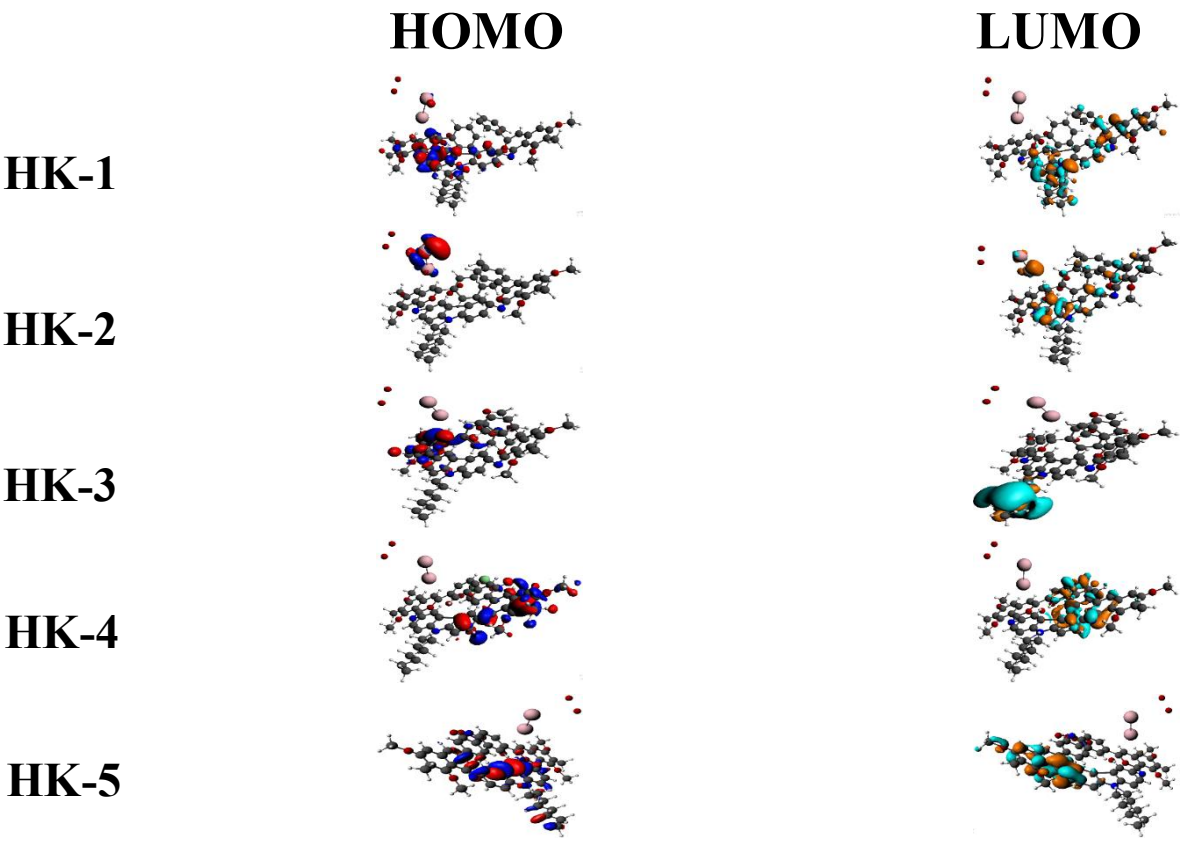

Fig 4.4: Computed isodensity surfaces of the HOMO and LUMO of the Hybrid dyes.

*Table 4.3: Electronic Parame*ters of Coumarin and Hybrid dyes

NO.	Coumarin			NO.	Coumarin-Carbazole Hybrid		
	E_{HOMO}	E_{LUMO}	ΔE		E_{HOMO}	E_{LUMO}	ΔE
C1	-0.4	0.73	-1.13	**HK-1**	-0.1	0.57	-0.67
C2	-0.35	0.4	-0.75	**HK-1**	-0.16	0.55	-0.71
C3	-0.7	1.3	-2.0	**HK-1**	-0.3	0.46	-0.76
C4	-0.36	0.9	-1.26	**HK-1**	0.17	0.83	-0.66
C5	-0.7	1.1	-1.8	**HK-1**	-0.45	0.72	-1.17

4.5 Electrochemical properties

Electrochemical investigations have been carried out using DFT on ADF to verify the thermodynamic probability of electron injection from the excited state of the dye to the conduction band of TiO_2 in DSSC. All these five target coumarins have reduction capabilities between -2.20 to 5.85 eV (Table: 4.4), whereas hybrid dyes have reduction aptitudes between -0.68 to 5.20 eV (Table: 4.5) that gives a better injection of the electron from LUMO to the conduction band of TiO_2 in DSSC.

Table 4.4: *Oxidation (E_{ox}), reduction (E_{red}), Fermi-level (E_0), and excited-state oxidation (E_{ox*}) of the coumarins adsorbed on titanium dioxide (TiO_2) used in DSSC.*

ENERGIES	COUM- (1)	COUM- (2)	COUM- (3)	COUM- (4)	COUM- (5)
E_{OX}	-0.4	-0.35	-0.7	-0.36	-0.7
E_{RED}	0.73	0.4	1.3	0.9	1.1
E_0	-0.565	-0.375	-1.0	-0.63	-0.9
E_{OX*}	0.165	0.025	0.3	0.27	0.2

Table 4.5: *Oxidation (E_{ox}), reduction (E_{red}), Fermi-level (E_0), and excited-state oxidation (E_{ox*}) of the hybrids adsorbed on titanium dioxide (TiO_2) used in DSSC.*

ENERGIES	HK-(1)	HK-(2)	HK-(3)	HK-(4)	HK-(5)
E_{OX}	-0.1	-0.16	-0.3	-0.17	-0.45
E_{RED}	0.57	0.55	0.46	0.83	0.72
E_0	-0.335	-0.355	-0.38	-0.33	-0.585
E_{OX*}	0.235	0.195	0.08	0.5	0.135

4.6 Comparison of Coumarin and Hybrid results

As a result, the interpretation showed that all hybrids have higher negative values after optimization compared with all coumarin dyes. Both hybrid and coumarin dyes are adsorbed via physisorption in DSSC, but hybrid dyes are most efficiently adsorbed as compared to coumarin dyes. On the other hand, hybrid dyes have better efficiency of injection of the electron from LUMO to the conduction band of TiO_2 than coumarin dyes in DSSC.

4.7 Discussion

Herein; we have analyzed that low efficiency of DSSC is attributed to the barrier of electron transfer from dye excited state to the conduction band of TiO_2. Inorganic dyes being used in DSSC tend to agglomerate due to reduction by electrolyte leading to poor functioning the DSSC. To stamp out the challenge, in this project we designed the D-π-A conjugated systems for carbazole-coumarin hybrids as dye conjugating system to be used as alternative of dye in DSSC. Periodic DFT calculations were carried out to understand the anchoring behavior of dyes and for carbazole-coumarin hybrids on theTiO_2 anatase surface. The lowest layer of the slab is fixed in this calculation in order to prevent the surface deformation. The calculated value of conduction band energy of TiO_2 is -0.1 eV. On the basis of adsorption energy for the adsorption of dye and hybrids, stability analysis revealed higher anchorage of hybrids as compared to dyes. Carbazole dye and coumarins were adsorbed a on the coordinated TiO_2 anatase surface in order to understand that how effectively these dyes remain stable on TiO_2. According to Table 4.1, the adsorption energy of carbazole is much better, favorably adsorbed, and showed stable interactions with TiO_2 Anatase surface. But according to table 4.2, adsorption energy for carbazole-coumarin hybrids, being more negative than the coumarins and carbazole disported feasible adsorption and firm interactions with TiO_2. The adsorption of coumarins, carbazole dye, and hybrids on TiO_2 anatase surface showed physio sorption behavior.

To evaluate the performance of TiO_2 based DSSC on the basis of difference in conduction band of TiO_2 and E_{ox*} of conjugated system (carbazole-coumarin hybrid), computational electrochemical investigations were performed to verify the excitation and injection tendency of electron from the excited state having energy E_{ox}^* of the carbazole-coumarin hybrid to the conduction band of TiO_2. According to frontier molecular orbitals, we have analyzed that hybrids can effectively inject electron into the conduction band of TiO2 facilitating flow of electrons in circuit. According to Table 4.4, coumarins and carbazole dye showed favorable distance between excited state of the dye and the conduction band of TiO_2. But due to the absence of D-π-A conjugated system in carbazole and coumarin dyes, they can be denaturalized and lower the lifetime and efficiency of the DSSC. In case of carbazole-coumarin hybrids, the distance between the excited state of the hybrids and conduction band is attainable and can perform effective injection of electron into the conduction band that can lead to increase the functioning and efficiency of DSSC.

To probe into electron transfer, electrical conductivity was then calculated for a carbazole dye and its hybrids with five coumarins, in which HK-1 showed viable conduction among all the hybrids and a carbazole dye due to having a low bandgap energy. Incident power conversion efficiency of fives hybrids was then compared with carbazole dye, and we came to know that HK-2 showed greatest efficiency of 21% among all the hybrids and a carbazole dye that is also the greatest efficiency than the till reported efficiency which is 14% for organic based dyes and 12% for inorganic based dyes attributed to high energy absorption of HK-2 at 58 nm (Near UV region) being reason for its higher excitation and injection of electrons into the conduction band of TiO2 It seems therefore crucial to setup a computational protocol able to study and optimize not only the properties (i.e., absorption and excitation) of the conjugated dye system but also the properties of the conjugated dye system -semiconductor interface.

Chapter 5

Conclusion & Future perspective

Chapter 5

Conclusions & Future Perspective

Conclusions

The development of efficient DSSC to compete with traditional silicon-based solar cells for the improvement of efficiency, stability, and commercialization is now underway. To add a contribution in this field E_{ox}, E_{red}, and E_{ox*} were evaluated out to explore the efficiency of electron injection into the conduction band of nanocrystalline TiO_2 from E_{LUMO} of the dye (photosensitizer) by using electron correlation methods. Here we validated the efficiency of hybrids over coumarins. Electronic parameters included the E_{ox} and E_{red} to identify the region of high and low electron density for electron transfer mechanism between hybrids and TiO_2. The determination of effective electron injection into the conduction band of TiO_2 is improved with the decrease of energy separation of E_{red} and the bottom of the TiO_2 conduction band. In the current research, the injection of an electron into the conduction band of TiO_2 from E_{red} of the hybrids is much efficient than the coumarins. The energy separation between the E_{red} of the hybrids and the conduction band of TiO_2 is much low as compared to coumarins except for hybrid (HK-2) that has high separation energy compared to the coumarin (coum-2).

The adsorption study revealed a significant result of contribution towards the adsorption of dye on nanocrystalline TiO_2 in DSSC and wider application towards renewable energy. The adsorption of coumarins, carbazole dye, and hybrids showed physisorption behavior. Due to the physisorption approach, there will be no demolishing of the dye (photosensitizer) and the electric current will be continuously created by the cell in the low light. Results revealed that dye-hybrids showed the greatest efficiency of electron injection into the conduction band of nanocrystalline TiO_2, over coumarins in the current research.

Future Perspectives

The photosensitizer is a crucial component of DSSC. To improve the cell's performance, it is critical to select an efficient dye. According to studies, the best dyes have electron-rich (donor) and electron-poor (acceptor) parts that are joined by a conjugated pi-bridge. The current research was made for the improvement of the structural design of donor pi-acceptor **(D- π A)** of dye in DSSC. Hybrids of carbazole dye and coumarins were designed for efficiency improvement in DSSC. The current research will be very helpful in the field of renewable energy for making more advanced solar panels in the future. Also, it will enhance the performance and efficiency of solar materials in material industries. Current research will be helpful in the field of material sciences, environmental sciences, and electronic industries for renewable energy.

References

[1] J. T. Houghton, G. J. Jenkins, and J. J. Ephraums, "Climate change: the IPCC scientific assessment," *Climate change: the IPCC scientific assessment*. 1990.

[2] B. Li, L. Wang, B. Kang, P. Wang, and Y. Qiu, "Review of recent progress in solid-state dye-sensitized solar cells," *Sol. Energy Mater. Sol. Cells*, vol. 90, no. 5, pp. 549–573, 2006.

[3] M. S. Dresselhaus and I. L. Thomas, "Alternative energy technologies. dresselhaus2001," *Nature*, vol. 414, no. 6861, pp. 332–337, 2001.

[4] D. M. Chapin, C. S. Fuller, and G. L. Pearson, "A new silicon p-n junction photocell for converting solar radiation into electrical power [3]," *J. Appl. Phys.*, vol. 25, no. 5, pp. 676–677, 1954.

[5] M. Kugelman, *Pakistan's Interminable Energy Crisis: Is There Any Way Out?* 2015.

[6] F. Hall and R. Greeno, "Alternative and Renewable Energy," *Build. Serv. Handb.*, pp. 641–660, 2019.

[7] Asif, M. (2009). Sustainable energy options for Pakistan. *Renewable and Sustainable Energy Reviews*, *13*(4), 903-909.

[8] T. S. M. Hamzah Rifaat, "The China-Pakistan Economic Corridor: Strategic Rationales, External Perspectives, and Challenges to Effective Implementation: An SAV Visiting Fellow Working Paper | Stimson Center," p. 3437, 2016.

[9] NEPRA, "State of Industry Report 2020," *Regulations*, vol. 53, no. 9, pp. 1689–1699, 2019.

[10] K. Tennakone, G. R. R. A. Kumara, I. R. M. Kottegoda, K. G. U. Wijayantha, and V. P. S. Perera, "A solid-state photovoltaic cell sensitized with a ruthenium bipyridyl complex," *J. Phys. D. Appl. Phys.*, vol. 31, no. 12, pp. 1492–1496, 1998.

[11] S. Lijima, "© 19 9 1 Nature Publishing Group 그라첼꺼," *Nature*, vol. 354, pp. 56–58, 1991.

[12] A. J. McEvoy and M. Grätzel, "Sensitisation in photochemistry and photovoltaics," *Sol. Energy Mater. Sol. Cells*, vol. 32, no. 3, pp. 221–227, 1994.

[13] G. Smestad, C. Bignozzi, and R. Argazzi, "Testing of dye sensitized TiO2 solar cells I: Experimental photocurrent output and conversion efficiencies (sol. energy mater. sol. cells 32 (1994) 259-272)," *Sol. Energy Mater. Sol. Cells*, vol. 33, no. 2, p. 253, 1994.

[14] K. Ranabhat, L. Patrikeev, A. A. evna Revina, K. Andrianov, V. Lapshinsky, and E. Sofronova, "An introduction to solar cell technology," *J. Appl. Eng. Sci.*, vol. 14, no. 4, pp. 481–491, 2016.

[15] REN21, *Renewables 2016 Global Status Report*. 2016.

[16] J. T. McLeskey and Q. Qiao, "Nanostructured organic solar cells," *Nanotechnol. Photovoltaics*, pp. 147–185, 2010.

[17] M. a Alam and B. Ray, "Lecture 5 Physics of Organic Solar Cells," *NCN Summer Sch. July 2011*, no. July, 2011.

[18] M. Demant, J. Greulich, M. Glatthaar, J. Haunschild, and S. Rein, “Modelling of physically relevant features in photoluminescence images,” *Energy Procedia*, vol. 27, pp. 247–252, 2012.

[19] P. Würfel, T. Trupke, T. Puzzer, E. Schäffer, W. Warta, and S. W. Glunz, “Diffusion lengths of silicon solar cells from luminescence images,” *J. Appl. Phys.*, vol. 101, no. 12, 2007.

[20] H. Kampwerth, T. Trupke, J. W. Weber, and Y. Augarten, “Advanced luminescence based effective series resistance imaging of silicon solar cells,” *Appl. Phys. Lett.*, vol. 93, no. 20, pp. 91–94, 2008.

[21] J. Kniepert, M. Schubert, J. C. Blakesley, and D. Neher, “Photogeneration and recombination in P3HT/PCBM solar cells probed by time-delayed collection field experiments,” *J. Phys. Chem. Lett.*, vol. 2, no. 7, pp. 700–705, 2011.

[22] J. Lorrmann, B. H. Badada, O. Inganäs, V. Dyakonov, and C. Deibel, “Charge carrier extraction by linearly increasing voltage: Analytic framework and ambipolar transients,” *J. Appl. Phys.*, vol. 108, no. 11, 2010.

[23] R. Hanfland, M. A. Fischer, W. Brütting, U. Würfel, and R. C. I. Mackenzie, “The physical meaning of charge extraction by linearly increasing voltage transients from organic solar cells,” *Appl. Phys. Lett.*, vol. 103, no. 6, 2013.

[24] S. Shakir *et al.*, “Electro-catalytic and structural studies of DNA templated gold wires on platinum/ITO as modified counter electrode in dye sensitized solar cells,” *J. Mater. Sci. Mater. Electron.*, vol. 29, no. 6, pp. 4602–4611, 2018.

[25] A. Hagfeldt, “Brief overview of dye-sensitized solar cells,” *Ambio*, vol. 41, no. SUPPL.2, pp. 151–155, 2012.

[26] G. Gordillo, “Photoluminescence and photoconductivity studies on ZnxCd1-xS thin films,” *Sol. Energy Mater. Sol. Cells*, vol. 25, no. 1–2, pp. 41–49, 1992.

[27] L. Finegold and J. L. Cude, “Biological sciences: One and two-dimensional structure of alpha-helix and beta-sheet forms of poly(L-Alanine) shown by specific heat measurements at low temperatures (1.5-20 K),” *Nature*, vol. 238, no. 5358, pp. 38–40, 1972.

[28] M. Grätzel, “PECreview,” *Nature*, vol. 414, no. November, pp. 338–344, 2001.

[29] H. Tributsch and H. Gerischer, “The use of semiconductor electrodes in the study of photochemical reactions,” *Berichte der Bunsengesellschaft für Phys. Chemie*, vol. 73, pp. 850–854, 1969.

[30] J. Desilvestro, M. Grätzel, L. Kavan, J. Moser, and J. Augustynski, “Highly Efficient Sensitization of Titanium Dioxide,” *J. Am. Chem. Soc.*, vol. 107, no. 10, pp. 2988–2990, 1985.

[31] K. Sharma, V. Sharma, and S. S. Sharma, “Dye-Sensitized Solar Cells: Fundamentals and Current Status,” *Nanoscale Res. Lett.*, vol. 13, 2018.

[32] M. L. Parisi, S. Maranghi, and R. Basosi, “The evolution of the dye sensitized solar cells from Grätzel prototype to up-scaled solar applications: A life cycle assessment approach,” *Renew. Sustain. Energy Rev.*, vol. 39, pp. 124–138, 2014.

[33] J. Jeevanandam, A. Barhoum, Y. S. Chan, A. Dufresne, and M. K. Danquah, “Review on nanoparticles and nanostructured materials: History, sources, toxicity and regulations,”

Beilstein J. Nanotechnol., vol. 9, no. 1, pp. 1050–1074, 2018.

[34] S. Thiyagu and N. Fukata, *Silicon nanowire-based solar cells*. Elsevier Inc., 2019.

[35] H. Panchal and K. Shah, "DYE SENSITIZED SOLAR CELLS -AN ALTERNATIVE TO SILICON BASED DYE SENSITIZED SOLAR CELLS - AN ALTERNATIVE TO SILICON BASED PHOTOVOLTAIC TECHNOLOGY Hardik Panchal *, Keval Shah , Mayur Padharia Abstract :," no. December, 2015.

[36] C. Anselmi, E. Mosconi, M. Pastore, E. Ronca, and F. De Angelis, "Adsorption of organic dyes on TiO 2 surfaces in dye-sensitized solar cells: Interplay of theory and experiment," *Phys. Chem. Chem. Phys.*, vol. 14, no. 46, pp. 15963–15974, 2012.

[37] E. A. M. Gad, E. M. Kamar, and M. A. Mousa, "Experimental and computational study on electronic and photovoltaic properties of chromen-2-one-based organic dyes used for dye-sensitized solar cells," *Egypt. J. Pet.*, vol. 29, no. 2, pp. 203–209, 2020.

[38] C. Sun, Y. Li, P. Song, and F. Ma, "An experimental and theoretical investigation of the electronic structures and photoelectrical properties of ethyl red and carminic acid for DSSC application," *Materials (Basel).*, vol. 9, no. 10, pp. 1–22, 2016.

[39] M. Hachi, A. Slimi, A. T. Benjelloun, A. Fitri, S. Elkhattabi, and M. Benzakour, "The influence of the structural variations in the π-bridge of D-π-A organic dyes on the efficiency of dye-sensitized solar cells (DSSCs): A DFT computational study," *2020 5th Int. Conf. Renew. Energies Dev. Countries, REDEC 2020*, no. August, 2020.

[40] J. Baldenebro-López, J. Castorena-González, N. Flores-Holguín, J. Almaral-Sánchez, and D. Glossman-Mitnik, "Computational molecular nanoscience study of the properties of copper complexes for dye-sensitized solar cells," *Int. J. Mol. Sci.*, vol. 13, no. 12, pp. 16005–16019, 2012.

[41] S. Fantacci, F. De Angelis, and A. Selloni, "Absorption spectrum and solvatochromism of the [Ru(4,4′-COOH-2,2′-bpy)2(NCS)2] molecular dye by time dependent density functional theory," *J. Am. Chem. Soc.*, vol. 125, no. 14, pp. 4381–4387, 2003.